Minimal Stencils for Monotony or Causality Preserving Discretizations of Anisotropic PDEs

Jean-Marie Mirebeau

Minimal Stencils for Monotony or Causality Preserving Discretizations of Anisotropic PDEs

Jean-Marie Mirebeau*

November 24, 2014

Abstract

We consider discretizations of anisotropic diffusion and of the anisotropic eikonal equation, on two dimensional cartesian grids, which preserve their structural properties: monotonicity of diffusion, causality of the eikonal equation. These two PDEs embed geometric information, in the form of a field of diffusion tensors and of a Riemannian metric respectively. Common knowledge is that, when these tensors are strongly anisotropic, monotonous or causal discretizations of these PDEs cannot be strictly local [MW53, SV01]: numerical schemes need to involve interactions between each point and the elements of a *stencil*, which is not limited to its immediate neighbors on the discretization grid. Using tools from discrete geometry we identify the smallest valid stencils, in the sense of convex hull inclusion. We also estimate, for a fixed condition number but a random tensor orientation, the worst case and average case radius of these minimal stencils, which is relevant for numerical error analysis.

1 Introduction

Diffusion is a linear Partial Differential Equation (PDE) satisfying a monotonicity property; discretization schemes which preserve this structure benefit from the discrete maximum principle [Wei98], a strong stability guarantee. The eikonal equation is the PDE formulation of an optimal control problem: finding the shortest exit path from a given domain. Discretization schemes which preserve its causal structure can be solved in one pass using the Fast Marching algorithm [Tsi95, SV01], which has a quasi-linear complexity. Motivation for structure preservation is therefore plentiful, and stems from theoretical as much as practical considerations. In this intention, a variety of numerical schemes have been developed; for instance and without exhaustivity [MW53, BOZ04, Obe06, Wei98, FM13] for anisotropic diffusion, and [SV01, AM11, Mir14] for anisotropic eikonal equations.

Non-isotropic PDEs have numerous applications, of which we can only give a glimpse. Anisotropic diffusion is required in porous media simulation [Dro14], or stochastic control [BOZ04], but is also fundamental in image processing [Wei98]. The Anisotropic eikonal equation is naturally required for trajectory planning, but is also relevant for seismic imaging [SV03], and extensively used in medical image segmentation [BC10]. When discretizing PDEs, anisotropy usually comes with technical difficulties. Indeed, monotone or causal numerical schemes cannot be strictly local, but need to introduce interactions between each point and a *stencil* of potentially distant neighbors [SV03, Koc95]. The objective of this paper is to provide a complete

*CNRS, University Paris Dauphine, UMR 7534, Laboratory CEREMADE, Paris, France.
ANR grant NS-LBR ANR-13-JS01-0003-01

qualitative and quantitative understanding of this non-locality, in the limited setting of two dimensional discretizations on cartesian grids: we identify the smallest stencils, in the sense of convex hull inclusion, and we sharply estimate their worst case and average radius. For clarity we focus in this introduction on anisotropic diffusion, postponing the eikonal PDE to §2.1. Note that minimal stencils were similarly identified in [BCM14] for the monotone discretization of two dimensional Monge-Ampere equations.

The contributions of this paper can be summarized as follows: Theorem 1.3 shows that the discretization of anisotropic diffusion introduced in [FM13] is generically[1] optimal in terms of locality, in two dimensions (the optimality of the three dimensional discretization presented in [Mir14] remains unclear). Theorem 2.3 states a similar result for the discretization of the anisotropic eikonal equation introduced in [Mir14]. We refer to [FM13, Mir14] for implementation details, extensive numerical studies, and practical comparisons with several competing methods. Theorem 1.5 provides quantitative average and worst case estimates of the size of the stencils used in these discretizations, which could be the starting point of a numerical error analysis.

Let $d \geq 1$ denote the space dimension (later specialized to $d = 2$), and let $\Omega \subseteq \mathbb{R}^d$ be a smooth open bounded domain, on which PDEs will be posed. We denote by S_d^+ the set of positive definite $d \times d$ matrices, and associate to each $D \in S_d^+$ the anisotropic norm $\|e\|_D := \sqrt{\langle e, De \rangle}$, $e \in \mathbb{R}^d$. The anisotropic diffusion PDE embeds geometric information, in the form a positive definite tensor field $\mathbf{D} \in C^0(\overline{\Omega}, S_d^+)$. The anisotropy ratio $\kappa(D)$ of D reflects how much the associated norm distorts distances; it is the square root of the condition number

$$\kappa(D) := \max_{\|u\|=\|v\|=1} \frac{\|u\|_D}{\|v\|_D} = \sqrt{\|D\|\|D^{-1}\|}, \qquad \kappa(\mathbf{D}) := \max_{x \in \overline{\Omega}} \kappa(\mathbf{D}(x)). \tag{1}$$

We consider two flavors of anisotropic diffusion, named divergence form and non-divergence form [BOZ04]: denoting by $\nabla^k u$ the tensor of k-th derivatives of a smooth $u : \overline{\Omega} \to \mathbb{R}$

$$\begin{cases} \partial_t u = \operatorname{div}(\mathbf{D}\,\nabla u) & \text{in } \Omega, \\ \langle \nabla u, \mathbf{D}\,\mathbf{n} \rangle = 0 & \text{on } \partial\Omega. \end{cases} \qquad \begin{cases} \partial_t u = \operatorname{Tr}(\mathbf{D}\,\nabla^2 u) & \text{in } \Omega, \\ u = 0 & \text{on } \partial\Omega. \end{cases} \tag{2}$$

$\operatorname{Tr}(A)$ denotes the trace of a matrix A, and $\mathbf{n}$ the exterior normal to $\partial\Omega$. In the non-linear variants of these PDEs, the diffusion tensor field $\mathbf{D}$ is not prescribed a-priori, but instead depends non-linearly on the solution u [Wei98, BOZ04]. We limit in this paper our attention to the discretization difficulties associated to the *anisotropy* of a fixed diffusion tensor $\mathbf{D}$, and not to a potential non-linearity[2]. Divergence form anisotropic diffusion (2, left) is the gradient flow (with respect to the L^2 metric) of an elliptic energy

$$\partial_t u = -\nabla \mathcal{E}_{\mathbf{D}}(u), \qquad \text{with } \mathcal{E}_{\mathbf{D}}(u) := \frac{1}{2} \int_\Omega \|\nabla u(x)\|^2_{\mathbf{D}(x)} dx. \tag{3}$$

On the other hand non-divergence form diffusion (2, right) reflects the evolution of the density of a stochastic process [BOZ04] of diffusivity $\mathbf{D}$, absorbed at the boundary $\partial\Omega$.

Finite differences discretizations of anisotropic diffusion [Wei98, BOZ04, FM13] are based upon decompositions of diffusion tensors as sums of rank one matrices, as introduced in the next definition. A set $V \subseteq \mathbb{R}^d$ is said symmetric iff for all $e \in V$ one has $-e \in V$. We denote by $e \otimes e$ the tensor product of a vector $e \in \mathbb{R}^d$ with itself, which is a positive semi-definite matrix.

[1] The generic correspondence between the constructions of this paper and those of [FM13, Mir14] immediately follow from the connection, see Theorem 3 in [CS92], between Voronoi vectors and obtuse superbases.

[2] Our results are thus irrelevant for *non-linear isotropic* diffusion $\partial_t u = \operatorname{div}(\lambda(u)u)$, with a non-linear scalar diffusivity $\lambda(u)\,\mathrm{Id}$, as in the model of Perona and Malik. (Confusingly, the Perona-Malik PDE is also often referred to as anisotropic diffusion, see [Wei98] for a discussion on terminology.)

Definition 1.1. *A D-diffusion stencil, where $D \in S_d^+$, is a finite symmetric set $V \subseteq \mathbb{Z}^d \setminus \{0\}$ for which there exists non-negative weights $(\gamma_e)_{e\in V}$ such that $D = \sum_{e\in V} \gamma_e e \otimes e$.*

A D-diffusion stencil is thus also a λD diffusion stencil, for any $\lambda > 0$, by rescaling the weights. Observing that $\mathrm{Id} = \sum_{i=1}^d e_i \otimes e_i$, where $(e_i)_{i=1}^d$ denotes the canonical basis of $\mathbb{R}^d$, we find that $\{e_1, \cdots, e_d, -e_1, \cdots, -e_d\}$ is an Id-diffusion stencil. The following discretizations of anisotropic diffusion coincide with the standard discretization of the Laplace operator $\Delta u = \mathrm{div}(\nabla u) = \mathrm{Tr}(\nabla^2 u)$ if one uses this decomposition of the identity tensor. Given a D-diffusion stencil V, one obtains at first order for small $\varepsilon > 0$

$$\varepsilon^{-2} \sum_{e\in V} \gamma_e \left(u(x+\varepsilon e) - u(x)\right)^2 \approx \sum_{e\in V} \gamma_e \langle \nabla u(x), e\rangle^2 = \nabla u(x) \cdot \left(\sum_{e\in V} \gamma_e e \otimes e\right) \cdot \nabla u(x) = \|\nabla u(x)\|_D^2. \tag{4}$$

We denoted scalar products by $\langle \cdot, \cdot \rangle$, and matrix vector products by "$\cdot$". The error term, in $\mathcal{O}(\varepsilon^2)$ for smooth u, is discussed in (9). Fix $\varepsilon > 0$ and introduce the discrete domain $X_\varepsilon := \Omega \cap \varepsilon\mathbb{Z}^d$. For each $x \in X_\varepsilon$ let $V(x)$ be a $\mathbf{D}(x)$ diffusion stencil, and let $(\gamma_e^x)_{e\in V(x)}$ be the corresponding weights. For $u : X_\varepsilon \to \mathbb{R}$, the discretization $\mathcal{E}_\varepsilon$ of the elliptic energy (3) is

$$\mathcal{E}_\varepsilon(u) := \frac{\varepsilon^{d-2}}{2} \sum_{x\in X_\varepsilon} \sum_{\substack{e\in V(x) \\ x+\varepsilon e \in X_\varepsilon}} \gamma_e^x (u(x+\varepsilon e) - u(x))^2, \qquad \text{written } \mathcal{E}_\varepsilon(u) = \frac{\varepsilon^d}{2} \langle u, A_\varepsilon u\rangle. \tag{5}$$

The semi-definite symmetric matrix A_ε, associated to this non-negative quadratic form, has a special structure: diagonal coefficients are non-negative, off-diagonal coefficients are non-positive, and lines (and columns) sum to 0. Choose a timestep $\Delta t > 0$ satisfying the CFL condition $\Delta t < 1/A_\varepsilon^*$, where A_ε^* is the largest diagonal coefficient of A_ε. Consider the following explicit scheme for divergence form anisotropic diffusion: given $u_0 : X_\varepsilon \to \mathbb{R}$, for all $k \geq 0$

$$\frac{u_{k+1} - u_k}{\Delta t} = -\varepsilon^{-d} \nabla \mathcal{E}_\varepsilon(u_k), \qquad \text{equivalently } u_{k+1} = (\mathrm{Id} - A_\varepsilon \Delta t) u_k.$$

The update matrix $\mathrm{Id} - A_\varepsilon \Delta t$ is stochastic by lines (and also columns incidentally), thus it satisfies the the desired maximum principle, and is non-expansive in the L^∞ norm. The non-divergence form (2, right) can be handled as well: for small $\varepsilon > 0$, again with an $\mathcal{O}(\varepsilon^2)$ error

$$\sum_{e\in V} \gamma_e \frac{u(x+\varepsilon e) - 2u(x) + u(x-\varepsilon e)}{\varepsilon^2} \approx \sum_{e\in V} \gamma_e e \cdot (\nabla^2 u(x)) \cdot e = \mathrm{Tr}(\nabla^2 u(x) \sum_{e\in V} \gamma_e e \otimes e) = \mathrm{Tr}(D\nabla^2 u(x)).$$

This defines a discretization of the operator $-\mathrm{Tr}(\mathbf{D}\,\nabla^2 u)$, that we denote $B_\varepsilon u$, where $u : X_\varepsilon \to \mathbb{R}$ is extended by 0 outside X_ε for Dirichlet conditions. Again, diagonal coefficients of B_ε are positive, off-diagonal coefficients are non-positive, and lines of B_ε have a non-negative sum. Choose a timestep $\Delta t > 0$ satisfying the CFL condition $\Delta t < 1/B_\varepsilon^*$, where B_ε^* is the largest diagonal coefficient of B_ε. Setting $u_{k+1} = (\mathrm{Id} - B_\varepsilon \Delta t) u_k$ we define a numerical scheme for non-divergence form anisotropic diffusion, satisfying the maximum principle and non-expansive in the L^∞ norm.

We give in Theorem 1.3 a construction of diffusion stencils, in two dimensions, which is optimal in terms of locality. For that purpose, we introduce elementary notions of lattice geometry, illustrated on Figure 1 and 2.

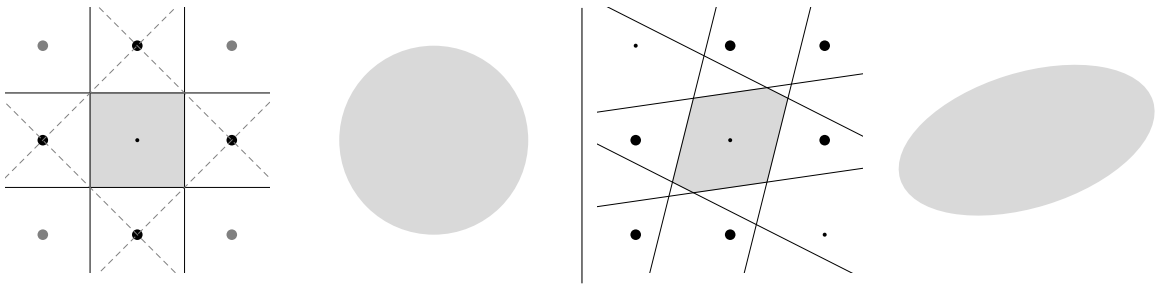

Figure 1: Voronoi geometry, and unit ball of $\|\cdot\|_M$, for to two matrices M. Left: $M = \mathrm{Id}$ (non generic case). Right: $M := M_\kappa(\theta)$, $\kappa = 1.4$, $\theta = 0.3$ (generic case), see (6). Gray polygon: Voronoi region $\mathrm{Vor}(M)$. Thick points: Voronoi vectors, strict ones in black, others in gray; in the generic second case, all Voronoi vectors are strict. Lines (dashed for non-strict Voronoi vectors) mark the equality $2\langle g, Me\rangle = \|e\|_M^2$; Voronoi facets $\mathrm{Vor}(M; e)$ are their intersections with the grayed Voronoi region $\mathrm{Vor}(M)$.

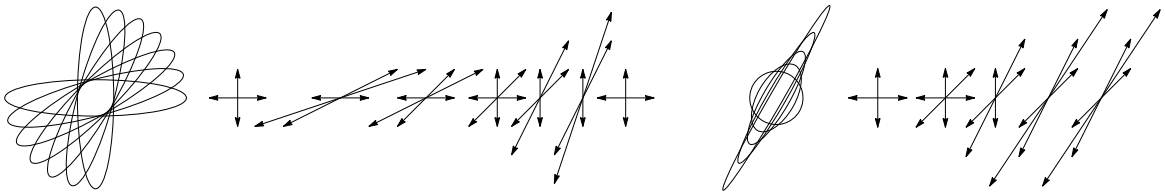

Figure 2: Unit circle $\{x; \|x\|_M = 1\}$, and collection of strict M-Voronoi vectors, for matrices $M = M(\kappa, \theta)$ of varying orientation (left: $\kappa = 5$, $\theta \in [0, \pi/2]$) or condition number (right: $\kappa \in [1, 16]$, $\theta = \pi/3$).

Definition 1.2. *For each matrix $M \in S_d^+$, we consider the Voronoi cell* $\mathrm{Vor}(M)$*, and facets* $\mathrm{Vor}(M; e)$*, $e \in \mathbb{Z}^d \setminus \{0\}$, defined by*

$$\mathrm{Vor}(M) := \{g \in \mathbb{R}^d;\ \forall e \in \mathbb{Z}^d,\ \|g\|_M \leq \|g - e\|_M\},$$
$$\mathrm{Vor}(M; e) := \{g \in \mathrm{Vor}(M);\ \|g\|_M = \|g - e\|_M\}.$$

An M-Voronoi vector is an element $e \in \mathbb{Z}^d \setminus \{0\}$ such that $\mathrm{Vor}(M; e) \neq \emptyset$*; it is said* strict *iff the facet* $\mathrm{Vor}(M; e)$ *is $(d-1)$-dimensional.*

For any $g, e \in \mathbb{R}^d$, one has $\|g\|_M \leq \|g - e\|_M \Leftrightarrow 2\langle g, Me\rangle \leq \|e\|_M^2$. Hence $\mathrm{Vor}(M)$ is a convex polytope, as an intersection of half-spaces. If e is a strict M-Voronoi vector then the exterior normal to the facet $\mathrm{Vor}(M; e)$ is Me.

Our next result characterizes two dimensional diffusion stencils which are *minimal* in the sense of convex hull inclusion. See Proposition 2.12 for the explicit stencil weights. Let $\mathrm{Hull}(V)$ denote the convex hull of a set $V \subseteq \mathbb{R}^d$.

Theorem 1.3. *Let $M \in S_2^+$ and let $D := M^{-1}$. The set V of strict M-Voronoi vectors is a D-diffusion stencil. Furthermore it is minimal in the following sense: any other D-diffusion stencil W satisfies* $\mathrm{Hull}(V) \subseteq \mathrm{Hull}(W)$.

The reason for the matrix inversion $D = M^{-1}$ in Theorem 1.3 is that the norm $\|\cdot\|_M$ is intended for measuring vectors, whereas the dual norm $\|\cdot\|_D$ is intended for measuring gradients (co-vectors). A three dimensional variant of this construction is presented in [FM13], as well as a comparison of the finite differences energy (5) with an alternative construction based on adaptive

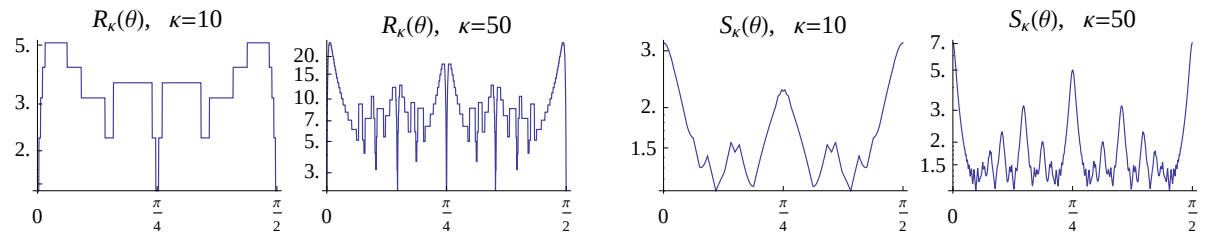

Figure 3: Plots of $R_\kappa(\theta)$ (left) and $S_\kappa(\theta)$ (right), for $\kappa \in \{10, 50\}$, as a function of $\theta \in [0, \pi/2]$. Logarithmic scale.

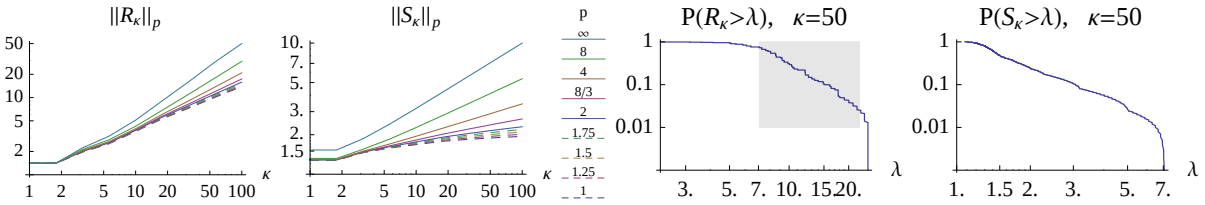

Figure 4: Left: L^p norms of R_κ and S_κ, as a function of $\kappa \in [1, 100]$ for different exponents $p \in [1, \infty]$. The behavior for $p < 2$ (dashed) and $p > 2$ is significantly different, see Theorem 1.5. Right: Tail distribution of R_κ and S_κ. Log-log scale.

finite elements. See also Remark 1 of [FM13] for a comparison with a simple alternative D-diffusion stencil, due to Weickert [Wei98], which (inevitably) is less local and efficient. Empirical experience indeed shows that the most robust and accurate PDE discretizations are typically achieved with the smallest stencils. Small stencils also limit discretization issues close to the domain boundary, and ease parallel implementations. In this light, Theorem 1.3 provides the best possible stencils for anisotropic diffusion, on two dimensional cartesian grids.

Our next result, Theorem 1.5 is a *quantitative* estimate of the size of D-diffusion stencils, which completes the *qualitative* optimality property of Theorem 1.3. For that purpose, we introduce some notation. Let $e^\perp := (-b, a)$ denote the rotation by $\pi/2$ of a vector $e = (a, b) \in \mathbb{R}^2$.

Definition 1.4. *For each $\kappa \in [1, \infty[$, $\theta \in \mathbb{R}$, we introduce the positive definite 2×2 matrix*

$$M_\kappa(\theta) := \kappa^{-1}\, e_\theta \otimes e_\theta + \kappa\, e_\theta^\perp \otimes e_\theta^\perp, \qquad \text{with } e_\theta := (\cos\theta, \sin\theta). \tag{6}$$

We denote by $V_\kappa(\theta)$ the collection of all strict $M_\kappa(\theta)$-Voronoi vectors, and define

$$R_\kappa(\theta) := \max_{e \in V_\kappa(\theta)} \|e\|, \qquad S_\kappa(\theta) := \max_{e \in V_\kappa(\theta)} \|e\|_{M_\kappa(\theta)}. \tag{7}$$

We allow ourselves a slight abuse of notation: "e_θ" always refers to the unit vector (6) of direction θ, although at times we introduce families $e_1, \cdots, e_r$ of vectors in $\mathbb{Z}^2$. Note that (6) is consistent with (1): $\kappa(M_\kappa(\theta)) = \kappa$.

The radius of M-diffusion stencils is measured through two different norms: the "extrinsic" euclidean norm (7, left), and the "intrinsic" $\|\cdot\|_{M_\kappa(\theta)}$-norm (7, right) tied to the anisotropic geometry embedded in the PDE. Both measures have their relevance and merits, as illustrated in a heuristic accuracy analysis of discretizations of the anisotropic eikonal PDE, Appendix B of [Mir14].

The maximum anisotropy ratio $\kappa(\mathbf{D})$, of the tensor field associated to an anisotropic PDE (1), is generally well known: it is problem data, reflecting a continuous model. In contrast we

regard the angle θ, between the cartesian grid axes and the preferred directions defined by the eigenvectors of $\mathbf{D}(x)$, $x \in \Omega$, as a random quantity uniformly distributed on $[0, \pi[$. In other words the preferred directions of the grid and of the PDE are viewed as independent of each other. This approach is tractable: although the dependence of $R_\kappa(\theta)$ and $S_\kappa(\theta)$ on θ is highly irregular (it depends on how well $\tan\theta$ is approximated by rationals), see Figure 3, direction independent quantities such as the $L^p([0,\pi[)$-norms of R_κ and S_κ depend smoothly on κ, see Figure 4. We underline quantities uniformly equivalent in κ with the notation

$$A(\kappa) \approx B(\kappa) \quad \Leftrightarrow \quad \exists C, c > 0,\ \forall \kappa \geq 1,\ cB(\kappa) \leq A(\kappa) \leq CB(\kappa). \tag{8}$$

Theorem 1.5. *For any $p \in [1, \infty]$ one has uniformly in κ (L^p norms are on the interval $[0, \pi[$)*

$$\|R_\kappa\|_{L^p} \approx \kappa^{\frac{1}{2}} \|S_\kappa\|_{L^p}. \qquad\qquad \|S_\kappa\|_{L^p} \approx \begin{cases} \kappa^{\frac{1}{2}-\frac{1}{p}} & \text{if } p > 2, \\ (\ln \kappa)^{\frac{1}{2}} & \text{if } p = 2, \\ 1 & \text{if } p < 2. \end{cases}$$

In applications, $\kappa(\mathbf{D}) = 10$ is already a pronounced anisotropy, and $\kappa(\mathbf{D}) = 100$ is presumably the most degenerate anisotropy that can conceivably be handled with the proposed discretization (5); for stronger anisotropies, more specialized approaches such as asymptotic preserving formulations [DLNN12] are recommended. Nevertheless Theorem 1.5 is a good indicator of the effective spread of our diffusion stencils, since the asymptotic behavior is quickly attained as shown on Figure 4. The proof in §3 is based on estimating the tail distributions of R_κ, S_κ.

Taking $p = \infty$ we obtain $R_\kappa(\theta) \leq C\kappa$, yet in the L^2 norm sense the stencil radius is closer to $\sqrt{\kappa \ln \kappa}$. The following heuristic analysis suggests that the L^2 norm of the stencil radius is indeed relevant for PDE numerical analysis. Consider $D \in S_d^+$, a D-diffusion stencil V with weights $(\gamma_e)_{e \in V}$, and a smooth u. Refining the approximation (4) we obtain

$$\varepsilon^{-2} \sum_{e \in V} \gamma_e (u(x + \varepsilon e) - u(x))^2 = \|\nabla u(x)\|_D^2 + \varepsilon^2 \sum_{e \in V} \gamma_e \Lambda(e, e, e, e) + \mathcal{O}(\varepsilon^4), \tag{9}$$

with the four-linear tensor $\Lambda = \nabla^2 u(x) \otimes \nabla^2 u(x) + 2\nabla u(x) \otimes \nabla^3 u(x)$. The second order $\mathcal{O}(\varepsilon^2)$ contribution is thus bounded by the three term product,

$$\sum_{e \in V} \gamma_e \|\Lambda\| \|e\|^4 \leq \|\Lambda\| \left(\sum_{e \in V} \gamma_e \|e\|^2 \right) \max_{e \in V} \|e\|^2 = \|\Lambda\| \operatorname{Tr}(D) r(V)^2.$$

involving a contribution $\|\Lambda\|$ of the PDE solution regularity, a contribution $\operatorname{Tr}(D)$ of the PDE data, and a contribution $r(V)^2$ from the scheme, where $r(V) := \max_{e \in V} \|e\|$ is the stencil radius. Consider the difference between the elliptic energy (3) and its discretization (5):

$$\begin{aligned} |\mathcal{E}_{\mathbf{D}}(u) - \mathcal{E}_\varepsilon(u)| \leq & \left| \int_\Omega \|\nabla u(x)\|_{\mathbf{D}(x)}^2 dx - \varepsilon^d \sum_{x \in X_\varepsilon} \|\nabla u(x)\|_{\mathbf{D}(x)}^2 \right| \\ & + \varepsilon^2 \left(\max_{x \in \Omega} \|\Lambda(x)\| \|\mathbf{D}(x)\| \right) \left(\varepsilon^d \sum_{x \in G_\varepsilon} r(V_x)^2 \right) + o(\varepsilon^2). \end{aligned}$$

The first contribution, a *quadrature* error, is scheme independent and expected to be $\mathcal{O}(\varepsilon^2)$ (at least for square domains, for which the boundary representation is exact). The second contribution, an $\mathcal{O}(\varepsilon^2)$ *discretization* error, is proportional to the average squared stencil radius, and thus tied to $\|R_\kappa\|_{L^2}$ estimated in Theorem 1.5.

Future research will be devoted to rigorous error analyses for anisotropic PDE discretizations with adaptive stencils, three dimensional counterparts of Theorem 1.3 and 1.5, and minimal stencils for other anisotropic PDEs.

Outline. We establish Theorem 1.3 in §2, as well as a similar result for the anisotropic eikonal equation. Theorem 1.5 is proved in §3.

2 Correctness and minimality of the proposed stencils

We present the anisotropic eikonal equation in §2.1, and describe its minimal causal stencils in Theorem 2.3. The correctness of and the minimality of these stencils is established in §2.2, while the similar results stated in the introduction for anisotropic diffusion are proved in §2.3.

2.1 The anisotropic eikonal equation

We introduce the *escape time problem*, and the eikonal PDE satisfied by its value function. We present its semi-Lagrangian discretization based on Pontryagin's principle, the concept of causal stencil, and identify the smallest such stencils. Let $\Omega \subseteq \mathbb{R}^d$ be an open bounded domain, and let $\mathbf{M} \in C^0(\overline{\Omega}, S_d^+)$ be a Riemannian metric. The Riemannian length of a Lipschitz path $\gamma : [0,1] \to \overline{\Omega}$, and the Riemannian distance between two points $x, y \in \overline{\Omega}$, are defined by

$$\begin{aligned}\text{length}(\gamma) &:= \int_0^1 \|\gamma'(t)\|_{\mathbf{M}(\gamma(t))} dt,\\ \text{dist}(x,y) &:= \min\{\text{length}(\gamma);\ \gamma \in \text{Lip}([0,1],\overline{\Omega}),\ \gamma(0) = x,\ \gamma(1) = y\}.\end{aligned}$$

Let $u(x)$ denote the escape time from $x \in \overline{\Omega}$: the length of the shortest path joining x to $\partial\Omega$. Let $x \in V \subseteq \Omega$. Pontryagin's principle, see Figure 5, accounts for the fact that any path joining x to $\partial\Omega$ does intersect ∂V

$$u(x) = \min_{y \in \partial V} \text{dist}(x,y) + u(y). \tag{10}$$

Choosing V as an infinitesimal ball containing x, one obtains that the value function u satisfies a partial differential equation. The Eikonal PDE, which must be understood in the sense of viscosity solutions [Lio82], reads with $\mathbf{D}(x) := \mathbf{M}(x)^{-1}$, $x \in \overline{\Omega}$

$$\begin{cases} \|\nabla u(x)\|_{\mathbf{D}(x)} = 1 & \text{for all } x \in \Omega,\\ u = 0 & \text{on } \partial\Omega. \end{cases} \tag{11}$$

The Hopf-Lax operator [SV03], introduced in the next definition, is a first order approximation of the right hand side of Pontryagin's principle (10). Let X denote a finite sampling of Ω, and let ∂X be a discrete representation of $\partial\Omega$.

Definition 2.1. *Associate to each $x \in X$ an hypersurface $V(x)$ (the* stencil *at x), enclosing x, and built of $(d-1)$-dimensional simplices with vertices in $X \cup \partial X$. The Hopf-Lax update operator reads: for each $x \in X$, $u : X \cup \partial X \to \mathbb{R}$*

$$\Lambda(u,x) := \min_{y \in V(x)} \|x - y\|_{\mathbf{M}(x)} + u(y), \tag{12}$$

where $u(y)$ is extended by piecewise linear interpolation to each facet of polygonal surface $V(x)$.

Note that the approximation $\text{dist}(x,y) \approx \|x-y\|_{\mathbf{M}(x)}$ amounts to regard the Riemannian metric $\mathbf{M}$ as constant within the stencil $V(x)$ of x, see Appendix B of [Mir14] for an heuristic

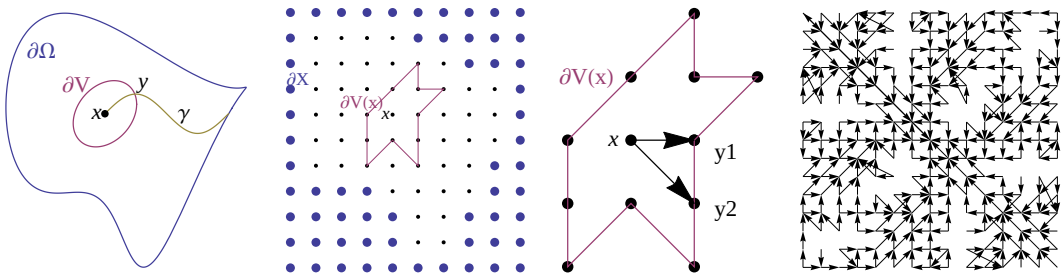

Figure 5: From left to right. I: Pontriagin's principle expresses that any path starting from x, and escaping Ω, must intersect ∂V at some point y. II: The fixed point discretization of the eikonal PDE approximates Pontryagin's principle, with point dependent stencils $V(x)$. III: The minimum defining $\Lambda(u,x)$ is attained on a facet of $\partial V(x)$, here a segment of endpoints y_1, y_2. IV: The *Causality property* guarantees that the resulting directed dependency graph is loop-less, so that the value function u can be evaluated in a single pass using the Fast-Marching algorithm.

error analysis. The Semi-Lagrangian discretization [SV03] of the eikonal equation (11) is a fixed point problem reflecting the identity (10): find $u : X \cup \partial X \to \mathbb{R}$ such that

$$\begin{cases} u(x) = \Lambda(u,x) & \text{for all } x \in X, \\ u(x) = 0 & \text{for all } x \in \partial X. \end{cases} \tag{13}$$

The shortest path problem on a graph admits a similar looking fixed point formulation, and can be solved through two methods: the fast, single pass Dijkstra $\mathcal{O}(N \ln N)$ algorithm provided all edge lengths are non-negative, or the slower Bellman-Ford $\mathcal{O}(N^2)$ algorithm which relaxes this condition, where N denotes the number of edges.

The graph connectivity underlying the system (13) depends on the discretization stencils $(V(x))_{x\in X}$, which are *not* fixed a priori and but may be freely chosen. A fundamental result of Sethian [SV03] is that if the stencils satisfy a geometrical acuteness condition, then the operator (12) obeys a *Causality property*, which is a counterpart of the the positivity of edge lengths in the graph setting.

Theorem 2.2 (Acuteness implies Causality, Sethian [SV03])**.** *Assume that for each $x \in X$, and any vertices y, y' of a common facet of $V(x)$ one has $\langle (y-x), \mathbf{M}(x)(y'-x)\rangle \geq 0$ (Acuteness condition). Let $y_1, \cdots, y_k$, $1 \leq k \leq d$, be the vertices of a minimal facet of $V(x)$ on which the minimum (12) is attained. Then $\Lambda(u,x) > u(y_i)$ for all $1 \leq i \leq k$ (Causality property).*

The causality property expresses that the discrete solution value $u(x) = \Lambda(u,x)$ only *effectively* depends on strictly smaller values $u(y_i)$, $1 \leq i \leq k$. The (Dijkstra-inspired) Fast Marching algorithm [Tsi95] reconstructs this ordering at run time, and thus solves the system (13) in a single pass of cost $\mathcal{O}(N \ln N)$. Without causality, some more robust but slower[3] Bellman-Ford inspired methods are available, such as [BR06] of cost $\mathcal{O}(N^{1+\frac{1}{d}})$.

The Acuteness condition is not only sufficient for Causality, but has also been shown to be necessary [Vla08]. Discretization stencils $(V(x))_{x\in X}$ with a large radius limit the accuracy of the discrete solution and raise boundary discretization issues. A natural objective is thus to find the smallest stencils satisfying the acuteness condition, hence also the causality property. Our next result states that strict $\mathbf{M}(x)$-Voronoi vectors define such a minimal stencil, for two dimensional cartesian grid discretizations.

[3] As pointed out in [BR06], a "slow" method with small stencils may in some cases terminate faster than a "fast" method with large stencils.

Theorem 2.3. *Assume that $d = 2$, $X = \Omega \cap \mathbb{Z}^2$, and $\partial X = \mathbb{Z}^2 \setminus X$. Let $x \in X$, let $e_1, \cdots, e_r$ be the strict $\mathbf{M}(x)$-Voronoi vectors sorted trigonometrically, and let $V(x)$ denote the closed polygonal curve of segments $[x + e_i, x + e_{i+1}]$, $0 \leq i < r$, $e_0 := e_r$. Then $V(x)$ satisfies the Acuteness condition. Furthermore one has* $\mathrm{Hull}(V(x)) \subseteq \mathrm{Hull}(W(x))$ *for any stencil $W(x)$ also satisfying this condition.*

This construction is extended to three dimensions in [Mir14], but optimality properties are then unclear. Applications often require replacing the Riemannian metric $\mathbf{M}$ with more general, and notably non-symmetric, Finsler metric; in that case an efficient stencil construction is presented in [Mir13], but optimality is unknown as well. An alternative construction of stencils satisfying the acuteness condition is presented in [AM11], but (inevitably) it is less local and accurate than the one of Theorem 2.3, see [Mir14] for a comparison. Theorem 2.3 is proved in the next subsection.

2.2 Correctness and minimality of eikonal stencils

We establish Theorem 2.3, stating the correctness and the minimality of Voronoi vector based stencils for the anisotropic eikonal equation. Our first step, in Theorem 2.5, is to reformulate this result by removing references to global objects such as the Riemannian metric $\mathbf{M}$ or the discretization set X.

Let $\mathrm{Cone}(V)$ denote the convex cone generated by a set $V \subseteq \mathbb{R}^2$, and let $\mathrm{Cone}(e_1, \cdots, e_n) := \mathrm{Cone}(\{e_1, \cdots, e_n\})$. We say that f, g are trigonometrically consecutive elements of a set $V \subseteq \mathbb{R}^2$ (abbreviated "$f, g \in V$ are trigonometrically consecutive") iff $\det(f, g) > 0$ and V does not intersect the interior of $\mathrm{Cone}(f, g)$. For each $e = (a, b) \in \mathbb{Z}^2$, we denote $\gcd(e) := \gcd(a, b)$.

Definition 2.4. *Let $M \in S_2^+$. An M-eikonal stencil is a finite set $V \subseteq \mathbb{Z}^2 \setminus \{0\}$ such that (a)* $\mathrm{Cone}(V) = \mathbb{R}^2$, *and (b) $\langle f, Mg \rangle \geq 0$ for any trigonometrically consecutive $f, g \in V$.*

Consider the setting of Theorem 2.3: $d = 2$, $X = \Omega \cap \mathbb{Z}^2$, $\partial X = \mathbb{Z}^2 \setminus X$. Let $x \in X$ and let $M := \mathbf{M}(x)$. Let V be an M-eikonal stencil in the sense of Definition 2.4, and let $e_1, \cdots, e_r$ be the elements of V sorted trigonometrically, with $e_0 := e_r$. Then the polygonal curve $V(x)$ of segments $[x + e_i, x + e_{i+1}]$, $0 \leq i < r$, clearly is a stencil in the sense of Definition 2.1, satisfying the Acuteness condition of Theorem 2.2. Conversely, if $V(x)$ is as such, then $V := \{y - x;\ y \text{ is a vertex of } V(x)\}$ satisfies Definition 2.4.

Theorem 2.5. *Let $M \in S_2^+$, and let V denote the collection of strict M-Voronoi vectors (ordered trigonometrically). Then V is an M-eikonal stencil, and for any other M-eikonal stencil W one has* $\mathrm{Hull}(V) \subseteq \mathrm{Hull}(W)$.

Theorem 2.5 states both the correctness and the minimality of our stencil construction. The rest of this section is devoted to its proof: correctness is established in Corollary 2.7, and minimality in Proposition 2.10.

Lemma 2.6. *Let $M \in S_d^+$, and let $e, f \in \mathbb{Z}^d$ be such that* $\mathrm{Vor}(M; e) \cap \mathrm{Vor}(M; f) \neq \emptyset$. *Then $\langle e, Mf \rangle \geq 0$.*

Proof. Consider $x \in \mathrm{Vor}(M; e) \cap \mathrm{Vor}(M; f)$. Then $\|x - (e + f)\|_M \geq \|x - e\|_M = \|x - f\|_M = \|x\|_M$. Thus, as announced

$$0 \leq \|x - (e + f)\|_M^2 - \|x - e\|_M^2 - \|x - f\|_M^2 + \|x\|_M^2 = 2\langle e, Mf \rangle. \qquad \square$$

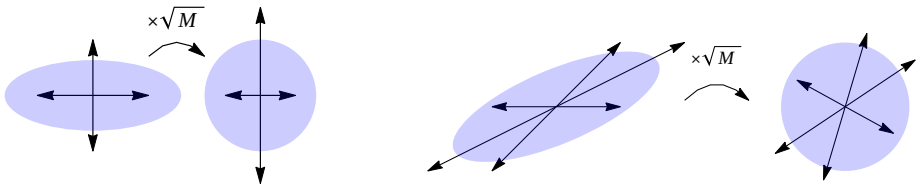

Figure 6: Unit ball $\{e; \|e\|_M \leq 1\}$ and collection of M-strict Voronoi vectors; same graphic after a linear change of coordinates by $M^{\frac{1}{2}}$. Left: diagonal matrix, Right: generic matrix. The angles of trigonometrically consecutive Voronoi vectors e, f are acute after the change of coordinates, as expected since $\langle e, Mf\rangle \geq 0$ by Corollary 2.7.

Corollary 2.7. *For any $M \in S_2^+$, the collection V of strict M-Voronoi vectors is an M-eikonal stencil. In particular, any trigonometrically consecutive $f, g \in V$ satisfy $\langle f, Mg\rangle \geq 0$.*

Proof. Recall that if $e \in V$, then the exterior normal to the edge $\mathrm{Vor}(M; e)$ is Me. Since the polygon $\mathrm{Vor}(M)$ has non-empty interior, the edge normals span: $\mathrm{Cone}(Me;\, e \in V) = \mathbb{R}^2$. Hence $\mathrm{Cone}(V) = \mathbb{R}^2$ as well, by linearity of M. Since M preserves orientation, for any trigonometrically consecutive $f, g \in V$ the sets $\mathrm{Vor}(M; f), \mathrm{Vor}(M; g)$ are consecutive edges of the polygon $\mathrm{Vor}(M)$. Hence they intersect, and thus $\langle f, Mg\rangle \geq 0$ by Lemma 2.6. □

We next turn to the minimality property of Theorem 2.5. Our first ingredient is an elementary arithmetic lemma, used in Corollary 2.9 to simplify the structure of M-eikonal stencils. We denote $[p_1, \cdots, p_n] := \mathrm{Hull}(\{p_1, \cdots, p_n\})$.

Lemma 2.8. *Let $(f, g) \in \mathbb{Z}^2$ be such that $|\det(f, g)| > 1$. Then the triangle $[0, f, g]$ contains a point $e \in \mathbb{Z}^2$ distinct from its vertices and such that $\gcd(e) = 1$.*

Proof. Since $|\det(f, g)| > 1$, the map $(\alpha, \beta) \in \mathbb{Z}^2 \mapsto \alpha f + \beta g \in \mathbb{Z}^2$ is not surjective. Hence there exists $(\alpha, \beta) \in \mathbb{Q}^2$, at least one of them non-integer, such that $\alpha f + \beta g \in \mathbb{Z}^2$. Up to replacing (α, β) with $(\alpha - m, \beta - n)$, $(m, n) \in \mathbb{Z}^2$, we may assume that $\alpha, \beta \in [0, 1]$. Up to replacing (α, β) with $(1-\alpha, 1-\beta)$, we may assume that $\alpha+\beta \leq 1$. The point $e := \alpha f+\beta g \in \mathbb{Z}^2$ belongs to T and is distinct from its vertices. In the case where $\gcd(e) > 1$, we can replace it with $e/\gcd(e)$. □

Corollary 2.9. *Let W be an M-eikonal stencil. Then there exists another M-eikonal stencil W' such that $\mathrm{Hull}(W') \subseteq \mathrm{Hull}(W)$ and $\det(f, g) = 1$ for any trigonometrically consecutive $f, g \in W'$.*

Proof. Define $W' := \{e \in \mathrm{Hull}(W) \cap \mathbb{Z}^2;\, \gcd(e) = 1\}$, and note that $\mathrm{Hull}(W') \subseteq \mathrm{Hull}(W)$. For each $e \in W$ one has $e' := e/\gcd(e) \in W'$, since $e' \in [0, e]$ and $0 \in \mathrm{Hull}(W)$ by point (a) of Definition 2.4. Hence $\mathrm{Cone}(W') = \mathrm{Cone}(W) = \mathbb{R}^2$, as required by point (a) of Definition 2.4.

Let $f', g' \in W'$ be trigonometrically consecutive. Then there exists $f, g \in W$ trigonometrically consecutive and such that $f', g' \in \mathrm{Cone}(f, g)$. From $\langle f, Mg\rangle \geq 0$ we get $\langle f', Mg'\rangle \geq 0$, as required by point (b) of Definition 2.4. Finally, one has $\det(f, g) > 0$ by definition, but also $|\det(f, g)| \leq 1$ by Lemma 2.8 and by construction of W'. Thus $\det(f, g) = 1$, as announced. □

Proposition 2.10. *For any M-eikonal stencil W, all strict M-Voronoi vectors belong to $\mathrm{Hull}(W)$.*

Proof. Let e be a strict M-Voronoi vector, and let f, g be trigonometrically consecutive elements of W such that $e \in \mathrm{Cone}(f, g)$. Then $e = \alpha f + \beta g$ for some $\alpha, \beta \in \mathbb{R}_+$. By Corollary 2.9 we can assume without loss of generality that $\det(f, g) = 1$, thus the vectors (f, g) form a basis of $\mathbb{Z}^2$, hence $\alpha, \beta \in \mathbb{Z}$. Since $\gcd(e) = 1$, one has $\gcd(\alpha, \beta) = 1$.

Assuming for contradiction that $\alpha, \beta \geq 1$ we obtain for any $p \in \mathbb{R}^2$

$$\begin{aligned}\alpha\|p-f\|^2 + \beta\|p-g\|^2 &= (\alpha+\beta)\|p\|^2 - 2\langle \alpha f + \beta g, p\rangle + \alpha\|f\|^2 + \beta\|g\|^2 \\ &= (\alpha+\beta-1)\|p\|^2 + \|p-e\|^2 - 2\alpha\beta\langle f, g\rangle.\end{aligned}$$

Since $\alpha\beta\langle f, g\rangle \geq 0$, and since $\alpha+\beta = (\alpha+\beta-1)+1$, it follows that $\min\{\|p-f\|, \|p-g\|\} \leq \max\{\|p\|, \|p-e\|\}$. Choosing p in the relative interior of $\mathrm{Vor}(M; e)$, so that the elements of $\mathbb{Z}^2$ closest to p are uniquely 0 and e, we obtain a contradiction. □

2.3 Correctness and minimality of diffusion stencils

We establish, as announced in Theorem 1.3, the correctness and the minimality of Voronoi-based D-diffusion stencils. Our first step is a description of the set of Voronoi vectors, which proof is postponed to Lemma 3.2 in §3.1.

Lemma 2.11. *For any $M \in S_2^+$, the collection V of strict M-Voronoi vectors has the form:*

- *(Non-Generic case) $V = \{e_1, e_2, -e_1, -e_2\}$, with $\det(e_1, e_2) = 1$ and $\langle e_1, Me_2\rangle = 0$.*
- *(Generic case) $V = \{e_0, -e_1, e_2, -e_0, e_1, -e_2\}$, with $e_0 + e_1 + e_2 = 0$, $\det(e_1, e_2) = 1$ and $\langle e_i, Me_j\rangle < 0$ for all $0 \leq i < j \leq 2$.*

We establish in the next proposition the *correctness* part of Theorem 1.3, by explicitly giving the positive weights mentioned in Definition 1.1 of diffusion stencils.

Proposition 2.12. *Let $M \in S_2^+$, $D := M^{-1}$, and let V denote the collection of strict M-Voronoi vectors. Then, distinguishing cases as in Lemma 2.11, one has (with cyclic indices)*

$$\text{(Non-generic case)} \qquad D = \sum_{1\leq i\leq 2} \|e_{i+1}^\perp\|_D^2 e_i \otimes e_i.$$

$$\text{(Generic case)} \qquad D = -\sum_{0\leq i\leq 2} \langle e_{i+1}^\perp, De_{i+2}^\perp\rangle e_i \otimes e_i.$$

Proof. The positivity of the weights $\|e_{i+1}^\perp\|_D^2$ is obvious in the non-generic case, while in the general case $-\langle e_{i+1}^\perp, De_{i+2}^\perp\rangle$ it follows from the positivity of $-\langle e_i, Me_j\rangle$ for distinct i, j, and from the identity: for any $f, g \in \mathbb{R}^2$

$$\langle f^\perp, Dg^\perp\rangle = \langle f, Mg\rangle / \det(M).$$

Let $f_i := e_i^\perp$, so that $\langle f_i, e_i\rangle = \langle e_i^\perp, e_i\rangle = 0$ and $|\langle f_i, e_j\rangle| = |\det(e_i, e_j)| = 1$ for any $i \neq j$. In the generic case, denoting by D' the right hand side, we check

$$\langle f_1, D'f_1\rangle = \|f_2\|_D^2\langle f_1, e_1\rangle^2 + \|f_1\|_D^2\langle f_1, e_2\rangle^2 = 0 + \|f_1\|_D^2 \times 1^2 = \langle f_1, Df_1\rangle.$$

Likewise $\langle f_1, D'f_2\rangle = \langle f_1, Df_2\rangle$ and $\langle f_1, D'f_2\rangle = 0 = \langle f_1, Df_2\rangle$. Thus $D' = D$ since (f_1, f_2) is a basis. In the generic case, denoting again by D' the right hand side, we have

$$\begin{aligned}-\langle f_0 D' f_0\rangle &= \langle f_1, Df_2\rangle\langle e_0, f_0\rangle^2 + \langle f_2, Df_0\rangle\langle e_1, f_0\rangle^2 + \langle f_0, Df_1\rangle\langle e_2, f_0\rangle^2 \\ &= \langle f_2, Df_0\rangle + \langle f_0, Df_1\rangle = \langle f_0, D(f_1+f_2)\rangle = -\langle f_0, Df_0\rangle.\end{aligned}$$

Likewise $\langle f_1, D'f_1\rangle = \langle f_1, Df_1\rangle$ and $\langle f_2, D'f_2\rangle = \langle f_2, Df_2\rangle$, hence $2\langle f_1, D'f_2\rangle = \langle f_0 D' f_0\rangle - \langle f_1, D'f_1\rangle - \langle f_2, D'f_2\rangle = 2\langle f_1, Df_2\rangle$ since $f_0 = -(f_1 + f_2)$. Since (f_1, f_2) is a basis we again obtain $D = D'$, which concludes the proof. □

We show in Corollary 2.14 that any D-diffusion stencil is also an M-diffusion stencil, with $M = D^{-1}$. The minimality of the collection of strict M-Voronoi vectors, as a D-diffusion stencil, thus follows from its minimality as an M-eikonal stencil, established §2.2. The correspondence of D-diffusion and M-eikonal stencils is specific to the two dimensional setting: their natural 3D counterparts [FM13, Mir14] are distinct, and do not have the same number of vertices.

Lemma 2.13. *Let $V \subseteq S^1 := \{e \in \mathbb{R}^2; \|e\| = 1\}$ be finite, symmetric w.r.t the origin, and let $(\gamma_e)_{e\in V}$ be non-negative weights such that $\sum_{e\in V} \gamma_e e \otimes e = \mathrm{Id}$. Then any trigonometrically consecutive $f, g \in V$ satisfy $\langle f, g\rangle \geq 0$.*

Proof. Claim: for any $\xi \in S^1$ there exists $e \in V$ such that $\langle \xi, e\rangle \geq 1/\sqrt{2}$. Indeed, since V is symmetric, we obtain otherwise $\langle \xi, e\rangle^2 < 1/2$ for all $e \in V$; but this implies the contradiction

$$1 = \|\xi\|^2 = \sum_{e\in V} \gamma_e \langle e, \xi\rangle^2 < \sum_{e\in V} \frac{\gamma_e}{2} = \frac{1}{2}\,\mathrm{Tr}\left(\sum_{e\in V} \alpha_e e \otimes e\right) = \frac{1}{2}\,\mathrm{Tr}(\mathrm{Id}) = 1.$$

Let $f, g \in V$ be trigonometrically consecutive, and let $\xi := (f+g)/\|f+g\|$. By construction $\langle \xi, f\rangle = \langle \xi, g\rangle \geq \langle \xi, e\rangle$ for all $e \in V$. Thus $1/\sqrt{2} \leq \langle \xi, f\rangle = \langle \xi, g\rangle$ by the above. Therefore the angle between f and g is at most $2\arccos(1/\sqrt{2}) = \pi/2$, which concludes the proof. □

Corollary 2.14. *Let $M \in S_2^+$ and let $D := M^{-1}$. Then any D-diffusion stencil is also an M-eikonal stencil. In particular, the collection of strict M-Voronoi vectors is a D-diffusion stencil which is minimal in the sense of convex hull inclusion.*

Proof. Let $V \subseteq \mathbb{Z}^2 \setminus \{0\}$ be symmetric, let $(\gamma_e)_{e\in V}$ be non-negative, and let us assume that $D = \sum_{e\in V} \gamma_e e \otimes e$. Note that $\mathrm{Cone}(V) = \mathbb{R}^2$, since D has full rank and V is symmetric.

Factorize $M = A^{\mathrm{T}}A$, and apply Lemma 2.13 to the vectors $\{Ae/\|Ae\|;\, e \in V\}$, and the weights $(\gamma_e\|Ae\|^2)_{e\in V}$. Then $0 \leq \langle Af, Ag\rangle = \langle f, Mg\rangle/(\|f\|_M^2\|g\|_M^2)$ for any trigonometrically consecutive $f, g \in V$. Thus $\langle f, Mg\rangle \geq 0$ and, as announced, we recognize an M-eikonal stencil. The minimality of the collection of strict M-Voronoi vectors follows from Theorem 2.5. □

3 Average norm of Voronoi vectors

We estimate the norm of $M_\kappa(\theta)$-Voronoi vectors, as announced in Theorem 1.5, for a fixed condition number κ^2, but in the $L^p([0,\pi[)$ sense over the anisotropy orientation θ. This type of result belongs to the well established field of lattice geometry, dating back to Lagrange [Lag75]. Lattice geometry field is currently the object of an important research activity, motivated by the numerous applications of the LLL algorithm [NV09] in particular in the field of cryptography. Nevertheless, the rather elementary Theorem 1.5 is original (to the author knowledge), for the following reasons:

(a) Research on lattice geometry is mainly focused on high dimensions.

(b) For many applications of current interest, such as cryptography, it is natural to assume that the lattice Gram matrix M has integer coefficients, in contrast with the present setting where $M = M_\kappa(\theta)$.

(c) The proposed random lattice model, which can be reformulated as $\Lambda = DR\mathbb{Z}^d$ with D diagonal of eigenvalues $\kappa^{\pm\frac{1}{2}}$ and R a random rotation, differs from classical [VV08] studies.

(d) The proposed result intertwines two mutually "singular" norms: the euclidean norm and the anisotropic $\|\cdot\|_M$ norm. Indeed we estimate the euclidean norm of M-Voronoi vectors. Research in lattice geometry in contrast commonly focuses on a single norm.

3.1 Reduced basis of a lattice

We introduce the concept of Minkowski basis [Ngu04], and use it to describe the set of M-Voronoi vectors and to derive uniform bounds on their norms. To each $M \in S_2^+$ we associate an $\|\cdot\|_M$-shortest non-zero vector $e_1(M) \in \mathbb{Z}^2$, and an $\|\cdot\|_M$-shortest linearly independent vector $e_2(M) \in \mathbb{Z}^2$

$$e_1(M) \in \operatorname*{argmin}_{e \in \mathbb{Z}^2 \setminus \{0\}} \|e\|_M, \qquad e_2(M) \in \operatorname*{argmin}_{f \in \mathbb{Z}^2 \setminus e_1(M)\mathbb{Z}} \|f\|_M. \tag{14}$$

The vectors $e_1(M)$ and $e_2(M)$ are uniquely determined, up to a change of sign, for all matrices M except a Lebesque negligible set. For non-generic matrices, an arbitrary minimizer is selected. In applications, the vectors (15) can be computed via Lagrange's algorithm [Ngu04], a generalization of Euclid's gcd algorithm. The next lemma shows that the two vectors (14) form a basis of $\mathbb{Z}^2$, often referred to as a Minkowski reduced basis [Ngu04].

Lemma 3.1 (Minkowski's vectors form a basis)**.** *Let $M \in S_2^+$ and let $e_i := e_i(M)$, $i \in \{1,2\}$. Then $\gcd(e_1) = \gcd(e_2) = 1$, and $|\det(e_1, e_2)| = 1$.*

Proof. One has $\gcd(e_1) = \gcd(e_2) = 1$, since otherwise the vector $e_i/\gcd(e_i)$ would violate the minimality property of e_i, $i \in \{1,2\}$, see (14). Since $e_2 \in \mathbb{Z}^2 \setminus e_1\mathbb{Z}$ and $\gcd(e_1) = 1$, the vectors e_1, e_2 are not collinear, hence $\det(e_1, e_2) \neq 0$. Assume for contradiction that $|\det(e_1, e_2)| > 1$ and, by Lemma 2.8, consider an element $e \in \mathbb{Z}^2$ of the triangle $[0, e_1, e_2]$ distinct from its vertices: $e = \alpha e_1 + \beta e_2$, $\alpha, \beta \geq 0$, $\alpha + \beta \leq 1$. Since $\gcd(e_1) = \gcd(e_2) = 1$, the vector e does not lie on an edge $[0, e_i]$, $i \in \{1,2\}$. Hence by the triangular inequality, which is strict since e_1, e_2 are not collinear and α, β are positive, we obtain $\|e\|_M < \alpha\|e_1\|_M + \beta\|e_2\|_M \leq \|e_2\|_M$. This contradicts the minimality of $\|e_2\|_M$, hence $|\det(e_1, e_2)| = 1$ which concludes the proof. □

Our next lemma describes the collection of strict M-Voronoi vectors, in terms of Minkowski's shortest vectors (14).

Lemma 3.2. *Let $M \in S_2^+$ and $e_i := e_i(M)$, $i \in \{1,2\}$. The set of strict M-Voronoi vectors is:*

- $\{\pm e_1, \pm e_2\}$ *if* $\langle e_1, Me_2\rangle = 0$.
- $\{\pm e_0, \pm e_1, \pm e_2\}$ *if* $\langle e_1, Me_2\rangle < 0$, *with* $e_0 := -(e_1 + e_2)$. *In addition* $\langle e_0, Me_1\rangle < 0$ *and* $\langle e_0, Me_2\rangle < 0$. *(In the case* $\langle e_1, Me_2\rangle > 0$, *replace* e_2 *with its opposite.)*

Proof. Case $\langle e_1, Me_2\rangle < 0$. One has $\|e_2\|_M^2 \leq \|e_2 + e_1\|_M^2$, by minimality (14) of $\|e_2\|_M$, hence $-2\langle e_1, Me_2\rangle \leq \|e_1\|_M^2$ by developing the squared norm. Denoting $e_0 := -(e_1 + e_2)$ we thus have $\langle e_0, Me_1\rangle = -\langle e_1, Me_2\rangle - \|e_1\|_M^2 \leq \langle e_1, Me_2\rangle < 0$, and likewise $\langle e_0, Me_2\rangle < 0$. For the record, such a triplet (e_0, e_1, e_2) of vectors is called a strict M-obtuse superbase [CS92, Mir14, FM13] .

From this point, we unite the proof of the two cases. Denote by W the set of strict M-Voronoi vectors, and assume w.l.o.g that $\det(e_1, e_2) = 1$. Let $n = 6$ and let $(f_1, \cdots, f_6) := (e_0, -e_1, e_2, -e_0, e_1, -e_2)$ (resp. $n = 4$ and $(f_1, \cdots, f_4) := (e_1, e_2, -e_1, -e_2)$). Note that $(f_1, \cdots, f_n)$ are sorted trigonometrically. One has $\langle f_i, Mf_{i+1}\rangle \geq 0$ for all $1 \leq i \leq n$, where indices are understood modulo n. Therefore $V := \{f_1, \cdots, f_n\}$ is an M-eikonal stencil, and thus $W \subseteq \mathrm{Hull}(V)$ by Proposition 2.10.

Since $|\det(f_i, f_{i+1})| = 1$, for all $1 \leq i \leq n$, one has $[0, f_i, f_{i+1}] \cap \mathbb{Z}^2 = \{0, f_i, f_{i+1}\}$ by Proposition 2.8. Hence $\mathrm{Hull}(V) \cap \mathbb{Z}^2 = \cup_{i=1}^6 [0, f_i, f_{i+1}] \cap \mathbb{Z}^2 = V \cup \{0\}$, thus $W \subseteq V$. Recalling that W is an M-eikonal stencil, see Corollary 2.7, and observing that $\langle f_i, Mf_{i+2}\rangle < 0$, for all $1 \leq i \leq n$, we find that the inclusion $W \subseteq V$ *cannot* be strict, which concludes the proof. □

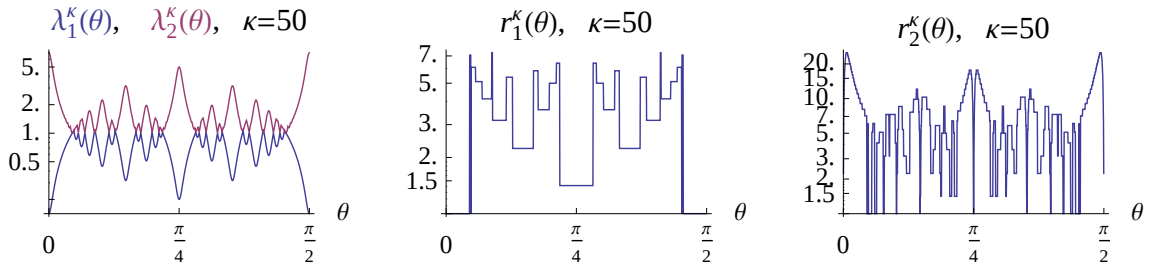

Figure 7: Minkowski minima λ_1^κ, λ_2^κ, and radii of Minkowski's vectors r_1^κ, r_2^κ. Logarithmic scale.

Our objective, Theorem 1.5, is to estimate the radius of the set of strict M-Voronoi vectors. In light of the previous lemma, we introduce for $M \in S_2^+$, $i \in \{1,2\}$, the norms

$$\lambda_i(M) := \|e_i(M)\|_M, \qquad r_i(M) := \|e_i(M)\|. \tag{15}$$

The scalars $\lambda_i(M)$ are called the Minkowski minima, and depend continuously on the matrix $M \in S_2^+$, in contrast with $r_i(M)$ and $e_i(M)$ which take discrete values. Minkowski minima are tied by Minkowski's second theorem [HW06], a fundamental result of lattice geometry stating that:

$$2 \le \frac{\pi}{\sqrt{\det M}} \lambda_1(M)\lambda_2(M) \le 4. \tag{16}$$

For each $\kappa \ge 1$, $\theta \in \mathbb{R}$, $i \in \{1,2\}$, we denote by $e_i^\kappa(\theta)$, $\lambda_i^\kappa(\theta)$, $r_i^\kappa(\theta)$, the vectors (14) and their norms (15) attached to the matrix $M_\kappa(\theta)$, defined in (6). Inequality (16) rewrites as

$$2/\pi \le \lambda_1^\kappa(\theta)\lambda_2^\kappa(\theta) \le 4/\pi. \tag{17}$$

This explains the approximate vertical symmetry in the plot of λ_1^κ, λ_2^κ, Figure 7 (left, log scale). We denote by $\measuredangle(f,g) \in [0,\pi/2]$ the unoriented angle between two vectors $f,g \in \mathbb{R}^2 \setminus \{0\}$, considered up to a change of sign:

$$\measuredangle(f,g) := \arccos\left(\frac{|\langle f,g\rangle|}{\|f\|\|g\|}\right) \in [0,\pi/2]. \tag{18}$$

Let $e \in \mathbb{R}^2 \setminus \{0\}$, let $\theta \in \mathbb{R}$, and let $\varphi = \measuredangle(e,e_\theta)$ where $e_0 := (\cos\theta, \sin\theta)$. Then

$$\|e\|_{M_\kappa(\theta)}^2 = \|e\|^2(\kappa \sin^2\varphi + \kappa^{-1}\cos^2\varphi), \qquad \text{hence } \kappa^{-\frac{1}{2}}\|e\| \le \|e\|_{M_\kappa(\theta)} \le \kappa^{\frac{1}{2}}\|e\|. \tag{19}$$

Lemma 3.3 (Uniform bounds on Minkowski's vectors)**.** *For any $\kappa \in [1,\infty[$, and any $\theta \in \mathbb{R}$ (omitting the argument θ for readability)*

$$\lambda_1^\kappa \in [\kappa^{-\frac{1}{2}}, c_1] \qquad \lambda_2^\kappa \in [c_2, \kappa^{\frac{1}{2}}],$$
$$r_1^\kappa \in [1, c_1\kappa^{\frac{1}{2}}] \qquad r_2^\kappa \in [1,\kappa],$$

where $c_1 := 2/\sqrt{\pi}$, $c_2 := \sqrt{2/\pi}$.

Proof. First line. Since $\lambda_1^\kappa \le \lambda_2^\kappa$ by construction, and $c_2^2 \le \lambda_1^\kappa\lambda_2^\kappa \le c_1^2$ by (17), we obtain $\lambda_1^\kappa \le c_1$ and $\lambda_2^\kappa \ge c_2$. By minimality (15) of $\|e_2^\kappa\|_{M_\kappa}$, and since at least one of the two independent vectors $(1,0)$ or $(0,1)$ is non-collinear with e_1^κ, one has $\lambda_2^\kappa = \|e_2^\kappa\|_{M_\kappa} \le \max\{\|(1,0)\|_{M_\kappa}, \|(0,1)\|_{M_\kappa}\} \le \kappa^{\frac{1}{2}} \max\{\|(1,0)\|, \|(0,1)\|\} = \kappa^{\frac{1}{2}}$ as anounced. The lower bound for λ_1^κ is shown below.

Second line. One has $1 \le \|e_1^\kappa\| =: r_1^\kappa$ since $e_1^\kappa \in \mathbb{Z}^2 \setminus \{0\}$, and likewise $r_2^\kappa \ge 1$. From (19, right) we obtain $\lambda_\kappa^1 \ge \kappa^{-\frac{1}{2}} r_1^\kappa \ge \kappa^{-\frac{1}{2}}$ which completes the first line, and $r_1^\kappa \le \kappa^{\frac{1}{2}}\lambda_1^\kappa \le c_1\kappa^{\frac{1}{2}}$ and $r_2^\kappa \le \kappa^{\frac{1}{2}}\lambda_2^\kappa \le \kappa$ which concludes the proof. □

Corollary 3.4. *With the notations of Lemma 3.3, one has for* $\kappa \geq c_1^2$

$$\frac{1}{2}R_\kappa \leq \max\{r_1^\kappa, r_2^\kappa\} \leq R_\kappa, \qquad \frac{1}{2}S_\kappa \leq \lambda_2^\kappa \leq S_\kappa, \tag{20}$$
$$R_\kappa \in [1, 2\kappa], \qquad S_\kappa \in [c_2, 2\kappa^{\frac{1}{2}}].$$

Proof. By Lemma 3.2, one has $\max\{r_1^\kappa, r_2^\kappa\} \leq R_\kappa \leq \max\{r_1^\kappa, r_2^\kappa, r_1^\kappa + r_2^\kappa\} \leq 2\max\{r_1^\kappa, r_2^\kappa\}$, as announced in (20, left). Proceeding likewise with $S_\kappa, \lambda_1^\kappa, \lambda_2^\kappa$, and observing that $\lambda_1^\kappa \leq \lambda_2^\kappa$ by construction (14), we obtain (20, right). The announced uniform bounds on R_κ, S_k, follow from those of Lemma 3.3. □

We introduce a set Z, where enumerates all rational directions in the plane

$$Z := \{e \in \mathbb{Z}^2;\, \gcd(e) = 1,\, e \succ (0,0) \text{ lexicographically}\}.$$

For any $e \in \mathbb{Z}^2 \setminus \{0\}$, the line $e\mathbb{R}$ intersects Z at a single point. Up changing their sign, we assume from this point that Minkowski's vectors $e_i(M)$, $i \in \{1,2\}$, $M \in S_2^+$, belong to Z. We end this subsection by estimating a sum, over pairs of co-prime integers, which repeatedly appears in the sequel.

Proposition 3.5. *One has*

$$\lim_{r\to\infty} \frac{\Sigma(r)}{r} = \frac{6}{\pi}, \qquad \text{where } \Sigma(r) := \sum_{e\in Z,\, \|e\|\leq r} \frac{1}{\|e\|}.$$

In particular, there exists $0 < c \leq C < \infty$ *such that* $cr \leq \Sigma(r) \leq Cr$ *for all* $r \geq 1$.

Proof. Let $p(r) := \#\{e \in \mathbb{Z}^2;\, 0 < \|e\| \leq r, \gcd(e) = 1\}/(\pi r^2)$ denote the relative density of points with co-prime coordinates in the ball of radius r. It is well known [HW79] that $g(r) \to 1/\zeta(2) = 6/\pi^2$ as $r \to \infty$. The announced result then follows from the observations

$$\frac{1}{\|e\|} = \int_{\|e\|}^r \frac{1}{s^2} ds + \frac{1}{r}, \qquad \text{hence } \frac{2\Sigma(r)}{\pi r} = \frac{1}{r}\int_0^r p(s)ds + p(r) = \frac{2}{\zeta(2)} + o(1). \qquad \square$$

3.2 Probabilistic estimate of the Minkowksi minima

We estimate the cumulative distribution of λ_1^κ, seen as a random variable of $\theta \in [0, \pi[$, for a fixed $\kappa \geq 1$, see Figure 9. Using Minkowski's second theorem (16), we infer the tail distribution of λ_2^κ. For that purpose we introduce the following angular sectors, illustrated on Figure 8 (left): for each $\kappa \geq 1$, $e \in Z$, $\alpha > 0$

$$\Phi_e^\kappa(\alpha) := \{\theta \in [0, \pi[;\, \sin \measuredangle(e, e_\theta) \leq \alpha/(\|e\|\sqrt{\kappa})\}.$$

Lemma 3.6. *Let* $\kappa \geq 1$, *let* $e \in Z$, *let* $\theta \in [0, \pi[$ *and let* $c > 0$. *We have the implications:*

$$\|e\|_{M_\kappa(\theta)} \leq c \;\Rightarrow\; \left(\theta \in \Phi_e^\kappa(c) \text{ and } \|e\| \leq c\sqrt{\kappa}\right) \;\Rightarrow\; \|e\|_{M_\kappa(\theta)} \leq c\sqrt{2}.$$

Proof. First implication. If $\|e\|_{M_\kappa(\theta)} \leq c$ then from (19, left), neglecting the contribution of $\kappa^{-1}\cos^2(\varphi)$, we obtain $\theta \in \Phi_e^\kappa(c)$. From (19, right) we get $\|e\| \leq c\sqrt{\kappa}$.

Second implication. Using again (19, left), we obtain:

$$\|e\|_{M_\kappa(\theta)}^2 \leq \|e\|^2 \left(\kappa\left(\frac{c}{\|e\|\sqrt{\kappa}}\right)^2 + \kappa^{-1}\right) = c^2 + \|e\|^2\kappa^{-1} \leq 2c^2. \qquad \square$$

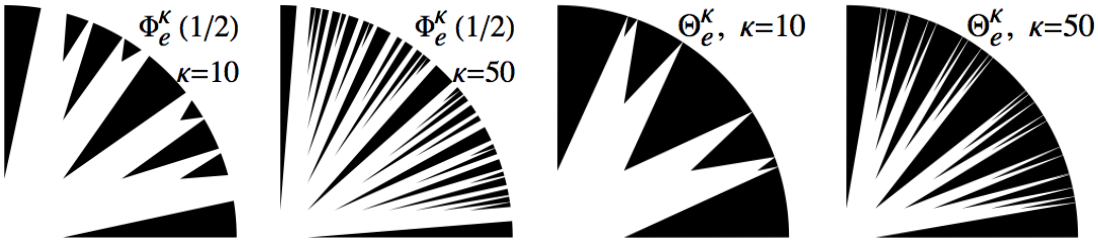

Figure 8: Left: representation of the sets $\Phi_e^\kappa(1/2)$, with $e \in Z$ and $\|e\| \leq \sqrt{\kappa}$. Right: sets Θ_e^κ. Each vector e is connected to corresponding angular sector on the circle.

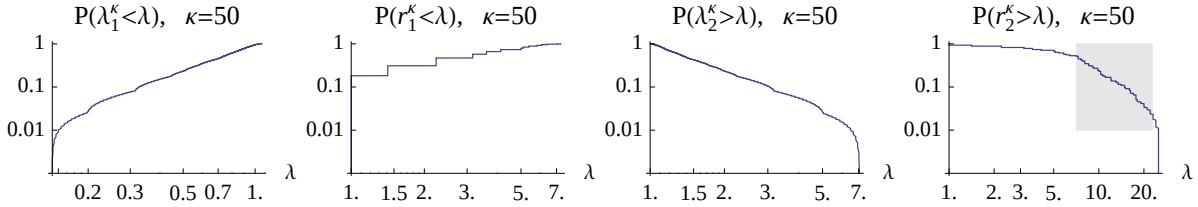

Figure 9: Cumulative distributions of λ_1^κ, r_1^κ, and tail distributions of λ_2^κ, r_2^κ. Log-log scales.

Corollary 3.7. *For any $\kappa \geq 1$, and any $\lambda \geq \kappa^{-\frac{1}{2}}$, one has with $\lambda' := \lambda/\sqrt{2}$*

$$\bigcup_{\substack{e\in Z\\ \|e\|\leq\lambda'\sqrt{\kappa}}} \Phi_e^\kappa(\lambda') \quad\subseteq\quad \{\theta\in[0,\pi[;\ \lambda_1^\kappa(\theta)\leq\lambda\} \quad\subseteq\quad \bigcup_{\substack{e\in Z\\ \|e\|\leq\lambda\sqrt{\kappa}}} \Phi_e^\kappa(\lambda). \tag{21}$$

Proof. The right implication in Lemma 3.6, with $c = \lambda' = \lambda/\sqrt{2}$, yields the first inclusion. The left implication in Lemma 3.6, with $c = \lambda$, yields the second inclusion. □

We estimate in Proposition 3.9 the distribution function $P(\lambda_1^\kappa \leq \lambda)$, by showing that the unions appearing in Corollary 3.7 are of disjoint sets. Probabilities considered here and in the following are for an uniformly distributed angle $\theta \in [0, \pi[$. We denote by $|E|$ the Lebesgue measure of a set $E \subseteq \mathbb{R}$. We recall that for any $\varphi \in]0, \pi/2]$ one has

$$\frac{2}{\pi}\varphi \leq \sin\varphi < \varphi. \tag{22}$$

Lemma 3.8. *Let $\kappa \geq 1$, and let $f, g \in Z$, $f \neq g$, be such that $\|f\|, \|g\| \leq c\sqrt{\kappa}$, with $c = 1/\pi$. Then $\Phi_f^\kappa(1) \cap \Phi_g^\kappa(1) = \emptyset$.*

Proof. Assume for contradiction that $\theta \in \Phi_f^\kappa(1) \cap \Phi_g^\kappa(1)$. Since f, g are distinct elements of Z, they are not collinear. Hence $\det(f, g) \neq 0$, and therefore $|\det(f, g)| \geq 1$ since this is a positive integer. We obtain using (22) the contradictory inequalities.

$$\begin{aligned}
\sphericalangle(f,g) \ &> \sin\sphericalangle(f,g) = \frac{|\det(f,g)|}{\|f\|\|g\|} \geq \frac{1}{\|f\|\|g\|}.\\
\sphericalangle(f,g) &\leq \sphericalangle(f,e_\theta) + \sphericalangle(e_\theta,g) \leq \frac{\pi}{2}(\sin\sphericalangle(f,e_\theta) + \sin\sphericalangle(e_\theta,g))\\
&\leq \frac{\pi}{2}\left(\frac{1}{\|f\|\sqrt{\kappa}} + \frac{1}{\|g\|\sqrt{\kappa}}\right) \leq \frac{\pi c}{\|f\|\|g\|}.
\end{aligned}$$

□

Proposition 3.9 (Cumulative distribution of λ_1^κ)**.** *There exists constants $C, c > 0$ such that: for all $\kappa \geq 1$, and all $\lambda \in [C\kappa^{-\frac{1}{2}}, c]$, one has $c\lambda^2 \leq P(\lambda_1^\kappa \leq \lambda) \leq C\lambda^2$.*

Proof. Let c_0 be the constant of Lemma 3.8, and let $\lambda' := \lambda/\sqrt{2}$. For $\lambda' \leq c_0$, the left term of (21) is a disjoint union. Hence we obtain successively, using (22) in the second line, and introducing Σ of Proposition 3.5 in the third

$$\begin{aligned}
\sum_{\substack{e\in Z\\ \|e\|\leq\lambda'\sqrt{\kappa}}} |\Phi_e^\kappa(\lambda')| \;\leq\; \pi P(\lambda_1^\kappa \leq \lambda) \;\leq\; \sum_{\substack{e\in Z\\ \|e\|\leq\lambda\sqrt{\kappa}}} |\Phi_e^\kappa(\lambda)|,\\
\sum_{\substack{e\in Z\\ \|e\|\leq\lambda'\sqrt{\kappa}}} \frac{\lambda'}{\|e\|\sqrt{\kappa}} \;\leq\; \pi P(\lambda_1^\kappa \leq \lambda) \;\leq\; \sum_{\substack{e\in Z\\ \|e\|\leq\lambda\sqrt{\kappa}}} \frac{\pi}{2}\frac{\lambda}{\|e\|\sqrt{\kappa}},\\
\frac{\lambda'}{\sqrt{\kappa}}\Sigma(\lambda'\sqrt{\kappa}) \;\leq\; \pi P(\lambda_1^\kappa \leq \lambda) \;\leq\; \frac{\pi}{2}\frac{\lambda}{\sqrt{\kappa}}\Sigma(\lambda\sqrt{\kappa}).
\end{aligned}$$

Assume in addition that $\lambda'\sqrt{\kappa} \geq 1$. Then denoting by c_1, C_1 the constants of Proposition 3.5

$$\frac{c_1}{2}\lambda^2 = \frac{\lambda'}{\sqrt{\kappa}}c_1\lambda'\sqrt{\kappa} \;\leq\; \pi P(\lambda_1^\kappa \leq \lambda) \;\leq\; \frac{\pi}{2}\frac{\lambda}{\sqrt{\kappa}}C_1\lambda\sqrt{\kappa} = \frac{\pi C_1}{2}\lambda^2.$$

This concludes the proof, with $c = \min\{c_0\sqrt{2}, c_1/(2\pi)\}$ and $C = \max\{\sqrt{2}, C_1/2\}$. □

Corollary 3.10 (Tail distribution of λ_2^κ)**.** *There exists constants $C, c > 0$ such that: for any $\kappa \geq 1$, and any $\lambda \in [C, c\kappa^{\frac{1}{2}}]$ one has $c\lambda^{-2} \leq P(\lambda_2^\kappa \geq \lambda) \leq C\lambda^{-2}$.*

Proof. The result follows from Proposition 3.9, and from (17) which implies for any $\lambda > 0$:

$$P(\lambda_1^\kappa \leq 2/(\lambda\pi)) \;\leq\; P(\lambda_2^\kappa \geq \lambda) \;\leq\; P(\lambda_1^\kappa \leq 4/(\lambda\pi)).$$ □

3.3 Euclidean norm of Minkowski's shortest vector

We estimate the distribution of the euclidean norm $r_1^\kappa(\theta)$ of Minkowski's vector $e_1^\kappa(\theta) \in Z$, defined as the shortest with respect to the anisotropic norm $\|\cdot\|_{M_\kappa(\theta)}$. For that purpose, we need to precisely identify this vector, hence we introduce for each $\kappa \geq 1$, $e \in Z$, the set

$$\Theta_e^\kappa := \{\theta \in [0, \pi[;\, e = e_1^\kappa(\theta)\},$$

Lemma 3.11. *Let $C = 2/\sqrt{\pi}$, $\kappa \geq 1$, and $e \in Z$. Then $\Theta_e^\kappa \subseteq \Phi_e^\kappa(C)$, and $\left(\Theta_e^\kappa \neq \emptyset \Rightarrow \|e\| \leq C\kappa^{\frac{1}{2}}\right)$.*

Proof. Using successively (i) the definition of Θ_e^κ, (ii) the uniform bound on $\lambda_1^\kappa(\theta)$ obtained in Lemma 3.3, for which $C = c_1$, and (iii) Lemma 3.6 (left implication) we obtain the implications

$$\theta \in \Theta_e^\kappa \Rightarrow \left(\|e\|_{M_\kappa(\theta)} = \lambda_1^\kappa(\theta)\right) \Rightarrow \left(\|e\|_{M_\kappa(\theta)} \leq C\right) \Rightarrow \left(\theta \in \Phi_e^\kappa(C) \text{ and } \|e\| \leq C\sqrt{\kappa}\right).$$

This establishes the announced inclusion and bound on $\|e\|$. □

Lemma 3.12. *Let $c < 1/(\pi\sqrt{2})$, let $\kappa \geq 1$, and let $e \in Z$. If $\|e\| \leq c\sqrt{\kappa}$ then $\Theta_e^\kappa \supseteq \Phi_e^\kappa(c)$.*

Proof. Let $\theta \in \Phi_e^\kappa(c)$, and $M := M_\kappa(\theta)$. By Lemma 3.6 (right implication) one has $\|e\|_M \leq c\sqrt{2}$.

Let $e' \in Z \setminus \{e\}$, and let $c_0 := 1/\pi$ be the constant from Lemma 3.8. If $\|e'\| \geq c_0\sqrt{\kappa}$, then $\|e'\|_M \geq \kappa^{-\frac{1}{2}}\|e'\| \geq c_0 > c\sqrt{2} \geq \|e\|_M$. On the other hand, if $\|e'\| \leq c_0\sqrt{\kappa}$, then $\Phi_e^\kappa(1) \cap \Phi_{e'}^\kappa(1)$ by Lemma 3.8. Thus $\theta \notin \Phi_{e'}^\kappa(1)$ and therefore, by $\|e'\|_M \geq 1 > c\sqrt{2} \geq \|e\|_M$ by Lemma 3.6 (left implication). We have shown that $\|e\|_M < \|e'\|_M$ for any $e' \in Z \setminus \{e\}$. Thus $e = e_1(M) = e_1^\kappa(\theta)$, in other words $\theta \in \Theta_e^\kappa$ as announced. □

We next estimate the distribution of r_1^κ. Strictly speaking this is not needed for the proof of Theorem 1.5, but we provide for completeness the argument, which is rather straightforward.

Proposition 3.13 (Cumulative distribution of r_1^κ)**.** *There exists $C, c > 0$ such that for any $\kappa \geq 1$ and any $\lambda \in [\kappa^{-\frac{1}{2}}, c]$, one has $c\lambda \leq P(r_1^\kappa \leq \lambda\sqrt{\kappa}) \leq C\lambda$.*

Proof. Let C_0 and c_0 denote the constants of Lemmas 3.11 and 3.12 respectively. For $\lambda \leq c_0$ one has

$$\sum_{\substack{e\in Z\\ \|e\|\leq\lambda\sqrt{\kappa}}} |\Phi_e^\kappa(c_0)| \leq \sum_{\substack{e\in Z\\ \|e\|\leq\lambda\sqrt{\kappa}}} |\Theta_e^\kappa| = \pi P(r_1^\kappa \leq \lambda\sqrt{\kappa}) \leq \sum_{\substack{e\in Z\\ \|e\|\leq\lambda\sqrt{\kappa}}} |\Phi_e^\kappa(C_0)|$$

Using (22) for the first line, and denoting by c_1, C_1 the constants of Proposition 3.5 for the second, we conclude for $\lambda\sqrt{\kappa} \geq 1$

$$\sum_{\substack{e\in Z\\ \|e\|\leq\lambda\sqrt{\kappa}}} \frac{c_0}{\|e\|\sqrt{\kappa}} \leq \pi P(r_1^\kappa \leq \lambda\sqrt{\kappa}) \leq \sum_{\substack{e\in Z\\ \|e\|\leq\lambda\sqrt{\kappa}}} \frac{\pi}{2}\frac{C_0}{\|e\|\sqrt{\kappa}}.$$

$$c_0c_1\lambda \leq c_0\frac{\Sigma(\lambda\sqrt{\kappa})}{\sqrt{\kappa}} \leq \pi P(r_1^\kappa \leq \lambda\sqrt{\kappa}) \leq \frac{C_0\pi}{2}\frac{\Sigma(\lambda\sqrt{\kappa})}{\sqrt{\kappa}} \leq \frac{C_0C_1\pi}{2}\lambda. \qquad \square$$

3.4 Euclidean norm of Minkowski's second shortest vector

We estimate the tail distribution of the euclidean norm $r_2^\kappa(\theta)$ of Minkowski's vector $e_2^\kappa(\theta)$, the second shortest with respect to the anisotropic norm $\|\cdot\|_{M_\kappa(\theta)}$. More precisely, our estimates account for the tail distribution behavior in the grayed region in Figure 9. Obtaining an upper bound is particularly simple, as shown in the next lemma.

Lemma 3.14 (Tail distribution of r_2^κ. Upper bound)**.** *There exists $C, c > 0$ such that for any $\kappa \geq 1$ and any $\lambda \in [C, c\kappa^{\frac{1}{2}}]$, one has $P(r_2^\kappa \geq \lambda\sqrt{\kappa}) \leq C\lambda^{-2}$.*

Proof. By (19, right) one has $r_2^\kappa(\theta) = \|e_2^\kappa(\theta)\| \leq \sqrt{\kappa}\|e_2^\kappa(\theta)\|_{M_\kappa(\theta)} = \lambda_2^\kappa(\theta)\sqrt{\kappa}$, for any $\kappa \geq 1$, $\theta \in \mathbb{R}$. Hence denoting by $C, c > 0$ the constants of Corollary 3.10 we obtain $P(r_2^\kappa \geq \lambda\sqrt{\kappa}) \leq P(\lambda_2^\kappa \geq \lambda) \leq C\lambda^{-2}$, for all $\lambda \in [C\kappa^{\frac{1}{2}}, c]$. $\square$

In order to estimate r_2^κ by below, we tie it to r_1^κ, a strategy similar to that used for the Minkowski minima λ_1^κ and λ_2^κ in §3.2. For any $\alpha \in \mathbb{R}$ we abusively denote $\alpha+\mathbb{Z} := \{\alpha+z;\, z \in \mathbb{Z}\}$

Lemma 3.15. *Let $M \in S_2^+$, let $e, f \in \mathbb{R}^d \setminus \{0\}$, let $\alpha \in \mathbb{R}$, and let k be a minimizer $\|f - ke\|_M$ in $\alpha + \mathbb{Z}$. Then $|k| + \frac{1}{2} \geq |\langle e, Mf\rangle|/\|e\|_M^2$.*

Proof. Up to a linear change of coordinates, we may assume that $M = \mathrm{Id}$. On the whole real line $\mathbb{R}$, the minimizer of $\lambda(l) := \|f - le\|^2 = \|f\|^2 - 2l\langle e, f\rangle + l^2\|e\|^2$ is $l := \langle f, e\rangle/\|e\|^2$. By symmetry and monotony of λ on both sides of l, we find that k is the (an) element of $(\alpha + \mathbb{Z})$ closest to l. Thus $|k - l| \leq \frac{1}{2}$, which concludes the proof. $\square$

Corollary 3.16. *Let $\kappa \geq 1$, $\theta \in \mathbb{R}$. Let us denote $e_1 := e_1^\kappa(\theta)$, $M := M_\kappa(\theta)$, and*

$$\mu_\kappa(\theta) := \frac{|\langle e_1, Me_1^\perp\rangle|}{\|e_1\|_M^2\|e_1\|^2}.$$

Then $r_2^\kappa(\theta) \geq r_1^\kappa(\theta)(\mu_\kappa(\theta) - 1/2)$.

Proof. Let $f := e_1^\perp/\|e_1\|^2$, let $e_2 := e_2^\kappa(\theta)$, and let us note that $|\det(e_1, e_2)| = 1 = \det(e_1, f)$. Up to replacing f with $-f$ we may thus assume that $\det(e_1, e_2 - f) = 0$. Therefore there exists $\alpha \in \mathbb{R}$ such that $e_2 = f - \alpha e_1$. For any $k \in \mathbb{R}$ one has ($f - ke_1 \in \mathbb{Z}^2$ iff $k \in \alpha + \mathbb{Z}$). By minimality (14) of $\|e_2\|_M$ among elements of $\mathbb{Z}^2$ non-collinear with e_1, we thus have $\|f - ke_1\|_M \geq \|f - \alpha e_1\|_M$ for any $k \in \alpha + \mathbb{Z}$. By Lemma 3.15

$$|\alpha| + \frac{1}{2} \geq |\langle e_1, Mf\rangle|/\|e_1\|_M^2 = \mu_\kappa(\theta).$$

Finally, $r_2^\kappa(\theta) = \|e_2\| = \|f - \alpha e_1\| \geq |\alpha|\|e_1\|$, since $\langle e_1, f\rangle = 0$, which concludes the proof. □

We study in Lemma 3.17 the angular sectors where $\mu_\kappa(\theta)$ is large, and deduce in Corollary 3.18 a lower bound on the tail distribution of r_2^κ, the counterpart of Lemma 3.14.

Lemma 3.17. *Let $\kappa \geq 1$, let $\lambda \in [C, \kappa^{\frac{1}{2}}]$, and let $e \in Z$ be such that $\lambda\|e\| \leq c\sqrt{\kappa}$. We denoted $C = 2$, $c = 1/8$. Then for all $e \in Z$ such that $\lambda\|e\| \leq c\sqrt{\kappa}$ one has*

$$|\{\theta \in \Theta_e^\kappa;\, \mu_\kappa(\theta) \geq \frac{\lambda\sqrt{\kappa}}{\|e\|}\}| \geq \frac{c}{\|e\|\lambda\sqrt{\kappa}}. \tag{23}$$

Proof. Let κ, λ, e be as in the lemma statement. Let $\theta \in [0, \pi[$ and let $\varphi = \sphericalangle(e_\theta, e)$. We define, and estimate using (19), the scalar

$$\mu := \frac{|\langle e, Me^\perp\rangle|}{\|e\|_M^2\|e\|^2} = \|e\|^{-2}\frac{(\kappa - \frac{1}{\kappa})\cos\varphi\sin\varphi}{\kappa\sin^2\varphi + \frac{1}{\kappa}\cos^2\varphi} = \|e\|^{-2}\frac{(\kappa^2 - 1)}{\kappa^2\tan\varphi + \operatorname{cotan}\varphi}. \tag{24}$$

One has the equivalence

$$\mu \geq \frac{\lambda\sqrt{\kappa}}{\|e\|} \quad \Leftrightarrow \quad \frac{\kappa^2 - 1}{\|e\|^2} \times \frac{\|e\|}{\lambda\sqrt{\kappa}} \geq \kappa^2\tan\varphi + \operatorname{cotan}\varphi. \tag{25}$$

Observe that $\kappa^2 - 1 \geq \kappa^2/2$, simplify powers and κ and $\|e\|$, and bound above the sum by twice its largest element. Then (25) is the consequence of the equivalent conditions.

$$\frac{\kappa^{\frac{3}{2}}}{2\lambda\|e\|} \geq 2\max\{\kappa^2\tan\varphi, \operatorname{cotan}\varphi\} \quad \Leftrightarrow \quad \tan\varphi \in \left[\frac{4\lambda\|e\|}{\kappa^{\frac{3}{2}}},\ \frac{1}{4\lambda\|e\|\kappa^{\frac{1}{2}}}\right] = \left[\frac{1}{\rho\kappa}, \frac{\rho}{\kappa}\right], \tag{26}$$

where we introduced the ratio $\rho := \frac{2c\sqrt{\kappa}}{\lambda\|e\|} \geq 2$. We assume the condition (26) and observe that

$$\sin\varphi \leq \tan\varphi \leq \frac{2c}{\lambda\|e\|\sqrt{\kappa}} \leq \frac{c}{\|e\|\sqrt{\kappa}},$$

thus $\theta \in \Phi_e^\kappa(c)$. By Lemma 3.12, and the assumption $\|e\| \leq c\sqrt{\kappa}$, we have $\Phi_e^\kappa(c) \subseteq \Theta_e^\kappa$. Thus $\theta \in \Theta_e^\kappa$, which implies $e = e_1^\kappa(\theta)$, and $\mu = \mu_\kappa(\theta)$. Denoting by I the interval (26), the measure (23) is thus at least

$$|\tan^{-1}(I)| + |\tan^{-1}(-I)| \geq 2\frac{1}{\kappa}\left(\rho - \frac{1}{\rho}\right) \times (\tan^{-1})'\left(\frac{\rho}{\kappa}\right) \geq \frac{\rho}{2\kappa}$$

We used the estimate $\rho \geq 2$, so that $\rho - \frac{1}{\rho} \geq \rho/2$; and $\frac{\rho}{\kappa} = \frac{2c}{\lambda\|e\|\sqrt{\kappa}} \leq \frac{c}{2}$ (since $\sqrt{\kappa} \geq \lambda \geq 2$ and $\|e\| \geq 1$) so that $(\tan^{-1})'(\rho/\kappa) = 1/(1 + (\rho/\kappa)^2) \geq 1/2$. This concludes the proof. □

Corollary 3.18 (Tail distribution of r_2^κ. Lower bound)**.** *There exists $0 < c \leq C < \infty$ such that for any $\kappa \geq 1$, and any $\lambda \in [C, c\kappa^{\frac{1}{2}}]$, one has $P(r_2^\kappa \geq \lambda\sqrt{\kappa}) \geq c\lambda^{-2}$.*

Proof. Let c_0, C_0 be the constants of Lemma 3.17, let κ, λ, e, satisfy the conditions of its statement, and let θ be in the set (23). Then $\mu_\kappa(\theta) \geq \lambda^2/c_0 \geq 1$, so that $\mu_\kappa(\theta) - 1/2 \geq \frac{1}{2}\mu_\kappa(\theta)$. We obtain, using Corollary 3.16 and since $r_1^\kappa(\theta) = \|e\|$

$$r_2^\kappa(\theta) \geq \|e\|(\mu_\kappa(\theta) - 1/2) \geq \frac{1}{2}\|e\|\mu_\kappa(\theta) \geq \frac{1}{2}\lambda\sqrt{\kappa}. \tag{27}$$

Denoting by c_1 and Σ the constant and function from Proposition 3.5, we conclude assuming $\lambda \leq c_0\sqrt{\kappa}$ for the last inequality

$$\begin{aligned} P(r_2^\kappa(\theta) \geq \frac{1}{2}\lambda\sqrt{\kappa}) &\geq \sum_{\substack{e\in Z \\ \|e\|\leq c_0\lambda^{-1}\sqrt{\kappa}}} |\{\theta \in \Theta_e^\kappa;\, \mu_\kappa(\theta) \geq \frac{\lambda\sqrt{\kappa}}{\|e\|}\}| \\ &\geq \sum_{\substack{e\in Z \\ \|e\|\leq c_0\lambda^{-1}\sqrt{\kappa}}} \frac{c_0}{\|e\|\lambda\sqrt{\kappa}} = \frac{c_0}{\lambda\sqrt{\kappa}}\Sigma(c_0\lambda^{-1}\sqrt{\kappa}) \geq c_0^2 c_1 \lambda^{-2}. \end{aligned}$$

□

3.5 Moments of the Voronoi radii

Concluding the proof of Theorem 1.5, we estimate the moments of the euclidean radius $R_\kappa(\theta)$ of the set of $M_\kappa(\theta)$-Voronoi vectors, and those of the "intrinsic" radius $S_\kappa(\theta)$. As usual the parameter $\kappa \geq 1$ is fixed, and the variable is $\theta \in [0, \pi[$. For that purpose, we combine the uniform bounds of Corollary 3.4 and estimates of their tail distribution.

Proposition 3.19. *There exists $C, c > 0$ such that for all $\kappa \geq 1$, and all $\lambda \in [C, c\kappa^{\frac{1}{2}}]$, one has*

$$c\lambda^{-2} \leq P(S_\kappa \geq \lambda) \leq C\lambda^{-2}, \qquad\qquad c\lambda^{-2} \leq P(R_\kappa \geq \lambda\kappa^{\frac{1}{2}}) \leq C\lambda^{-2}.$$

Proof. For readability, we omit the argument $\theta \in [0, \pi[$ of the functions involved. The estimate for S_κ immediately follows from the equivalence $S_\kappa/2 \leq \lambda_2^\kappa \leq S_\kappa$, see Corollary 3.4, and from the similar estimate for λ_2^κ, see Corollary 3.10. Regarding R_κ we have $R_\kappa/2 \leq \max\{r_1^\kappa, r_2^\kappa\} \leq R_\kappa$, but $r_1^\kappa \in [1, c_1\kappa^{\frac{1}{2}}]$ by Lemma 3.3. Hence, assuming $C > 2c_1$, we obtain for $\lambda \geq C$ the implications

$$R_\kappa \geq \lambda\kappa^{\frac{1}{2}} \;\Rightarrow\; \max\{r_1^\kappa, r_2^\kappa\} \geq \frac{1}{2}\lambda\kappa^{\frac{1}{2}} > c_1\kappa^{\frac{1}{2}} \geq r_1^\kappa \;\Rightarrow\; \max\{r_1^\kappa, r_2^\kappa\} = r_2^\kappa \;\Rightarrow\; R_\kappa/2 \leq r_2^\kappa \leq R_\kappa.$$

The announced estimate for $P(R_\kappa \geq \lambda\kappa^{\frac{1}{2}})$ then follows from the similar estimate for r_2^κ obtained in Lemma 3.14 and Corollary 3.18. □

In particular one has $P(S_\kappa \geq c\kappa^{\frac{1}{2}}) > 0$ for all $\kappa \geq (C/c)^2$, but we also know that $S_\kappa \leq 2\kappa^{\frac{1}{2}}$ by Corollary 3.4. Hence $\|S_\kappa\|_{L^\infty([0,\pi[)} \approx \kappa^{\frac{1}{2}}$ as announced in Theorem 1.5. For a finite exponent $p \in [1, \infty[$, one has

$$\frac{1}{\pi}\|S_\kappa\|_{L^p([0,\pi[)}^p = \frac{1}{\pi}\int_0^\pi S_\kappa^p(\theta)d\theta = p\int_0^\infty P(S_\kappa \geq \lambda)\lambda^{p-1}d\lambda \tag{28}$$

In view of the uniform bounds $S_\kappa \in [c_2, 2\kappa^{\frac{1}{2}}]$ of Corollary 3.4, and of the estimates of Proposition 3.19 which hold over a range $[C, c\kappa^{\frac{1}{2}}]$, we cut the integration range $]0, \infty[$ of (28, right) into four sub-intervals. Assuming without loss of generality that $c_2 \leq C$, $c \leq 2$, and $\kappa \geq (C/c)^2$

$$I_1 :=]0, C[,\; I_2 := [C, c\kappa^{\frac{1}{2}}[,\; I_3 := [c\kappa^{\frac{1}{2}}, 2\kappa^{\frac{1}{2}}[,\; I_4 := [2\kappa^{\frac{1}{2}}, \infty[.$$

Interval I_4 does contribute to the integral (28). Since I_1 is bounded independently of κ, its contribution to (28) also is. Since the tail distribution $P(S_\kappa \geq \lambda)$ is decreasing in λ, the contribution to (28) of $I_3 = [\lambda_-, \lambda_+]$ is bounded by $C\lambda_-^{-2}\lambda_+^{p-1}(\lambda_+ - \lambda_-) \leq Cc^{-2}\kappa^{\frac{p}{2}-1}$. Finally, and most importantly, the contribution of I_2 is

$$p\int_C^{c\kappa^{\frac{1}{2}}} P(S_\kappa \geq \lambda)\lambda^{p-1}d\lambda \approx \int_C^{c\kappa^{\frac{1}{2}}} \lambda^{p-3}d\lambda \approx \begin{cases} 1 & \text{if } p < 2, \\ \ln\kappa & \text{if } p = 2, \\ \kappa^{\frac{p}{2}-1} & \text{if } p > 2, \end{cases}$$

for sufficiently large κ, with equivalence constants (8) depending only on p. This implies the estimate on $\|S_\kappa\|_{L^p([0,\pi[)}$ announced in Theorem 1.5. The case of $\|R_\kappa\|_{L^p([0,\pi[)}$ is analogous.

References

[AM11] Ken Alton and Ian M Mitchell. An Ordered Upwind Method with Precomputed Stencil and Monotone Node Acceptance for Solving Static Convex Hamilton-Jacobi Equations. *Journal of Scientific Computing*, 2011.

[BC10] Fethallah Benmansour and Laurent D. Cohen. Tubular Structure Segmentation Based on Minimal Path Method and Anisotropic Enhancement. *International Journal of Computer Vision*, 2010.

[BCM14] Jean-David Benamou, Francis Collino, and Jean-Marie Mirebeau. Monotone and Consistent discretization of the Monge-Ampere operator. *arXiv.org*, 2014.

[BOZ04] J Frederic Bonnans, Elisabeth Ottenwaelter, and Hasnaa Zidani. A fast algorithm for the two dimensional HJB equation of stochastic control. Technical report, 2004.

[BR06] Folkmar Bornemann and Christian Rasch. Finite-element Discretization of Static Hamilton-Jacobi Equations based on a Local Variational Principle. *Computing and Visualization in Science*, 2006.

[CS92] J H Conway and N J A Sloane. Low-Dimensional Lattices. VI. Voronoi Reduction of Three-Dimensional Lattices. *Proceedings of the Royal Society A: Mathematical, Physical and Engineering Sciences*, 1992.

[DLNN12] Pierre Degond, Alexei Lozinski, Jacek Narski, and Claudia Negulescu. An asymptotic-preserving method for highly anisotropic elliptic equations based on a micro-macro decomposition. *Journal of Computational Physics*, 2012.

[Dro14] Jérôme Droniou. Finite volume schemes for diffusion equations: Introduction to and review of modern methods. *Mathematical Models and Methods in Applied Sciences*, 2014.

[FM13] Jérôme Fehrenbach and Jean-Marie Mirebeau. Sparse Non-negative Stencils for Anisotropic Diffusion. *Journal of Mathematical Imaging and Vision*, 2013.

[HW79] GGH Hardy and E M Wright. *An Introduction to the Theory of Numbers*. Oxford Science Publications, 1979.

[HW06] Martin Henk and Jorg M. Wills. Minkowski's successive minima. *Univ., Fak. für Mathemathik*, 2006.

[Koc95] Maciej Kocan. Approximation of viscosity solutions of elliptic partial differential equations on minimal grids. *Numerische Mathematik*, 1995.

[Lag75] Joseph Louis Lagrange. *Recherches d'arithmétique*. CF Voss, 1775.

[Lio82] Pierre-Louis Lions. *Generalized solutions of Hamilton-Jacobi equations*. Pitman Boston, 1982.

[Mir13] Jean-Marie Mirebeau. Efficient fast marching with Finsler metrics. *Numerische Mathematik*, 2013.

[Mir14] Jean-Marie Mirebeau. Anisotropic Fast-Marching on cartesian grids using Lattice Basis Reduction. *SIAM Journal on Numerical Analysis*, 2014.

[MW53] T S Motzkin and W Wasow. On the approximation of linear elliptic differential equations by difference equations with positive coefficients. *J. Math. Physics*, 1953.

[Ngu04] P Nguyen. Low-dimensional lattice basis reduction revisited. *Algorithmic Number Theory*, 2004.

[NV09] Phong Q. Nguyen and Brigitte Vallée, editors. *The LLL Algorithm*. Springer Berlin Heidelberg, 2009.

[Obe06] A M Oberman. Convergent Difference Schemes for Degenerate Elliptic and Parabolic Equations: Hamilton–Jacobi Equations and Free Boundary Problems. *SIAM Journal on Numerical Analysis*, 2006.

[SV01] J. A. Sethian and A. Vladimirsky. Ordered upwind methods for static Hamilton-Jacobi equations. *Proceedings of the National Academy of Sciences of the United States of America*, 2001.

[SV03] James A. Sethian and Alexander Vladimirsky. Ordered upwind methods for static Hamilton-Jacobi equations: theory and algorithms. *SIAM Journal on Numerical Analysis*, 2003.

[Tsi95] J.N. Tsitsiklis. Efficient algorithms for globally optimal trajectories. *IEEE Transactions on Automatic Control*, 1995.

[Vla08] Alexander Vladimirsky. Label-setting methods for Multimode Stochastic Shortest Path problems on graphs. *Mathematics of Operations Research*, 2008.

[VV08] B Vallée and A Vera. Lattice reduction in two dimensions: analyses under realistic probabilistic models. In *DMCTS Proceedings*, 2008.

[Wei98] Joachim Weickert. *Anisotropic diffusion in image processing*. Teubner Stuttgart, 1998.